

## RESEARCH ARTICLE

# A multi-scaling approach showing a transient metabolic mismatch in a freshwater fish (*Zingel asper*) during an acute heat stress

Julia Watson<sup>1,\*</sup>, Chloé Souques<sup>1,\*</sup>, François-Xavier Dechaume-Moncharmont<sup>1</sup>, Damien Roussel<sup>1</sup>, Julie Le Guyader<sup>1</sup>, Rémy Lassus<sup>2</sup>, Ludovic Guillard<sup>1</sup>, Angeline Clair<sup>1,3</sup>, Laëtitia Averty<sup>3</sup>, Candice Bastianini<sup>1,3</sup>, Lilian Redon<sup>1</sup>, Anne Morales-Montaron<sup>1</sup>, Yann Voituron<sup>1</sup>, Martin Daufresne<sup>2</sup>, Elisa Thorald<sup>4,5</sup> and Loïc Teulier<sup>1,‡</sup>

## ABSTRACT

Heat stress events will be more frequent and intense in the future. These events will challenge the capacity of organisms to exhibit sufficient metabolic flexibility to adapt to such variations. To better understand the acclimation processes implemented in response to acute warming, with an integrative approach we examined *in vivo* metabolic rate and cardiac mitochondrial respiration in the Rhône streber, during and after a heat stress on a precise time line. The temperature was raised from 13°C to 18°C (+1°C per hour) and maintained at 18°C for 5 days, before returning to 13°C at the same rate. We repeatedly measured, during the heat stress and 5 days after the end of the event, *in vivo* metabolic rate in the same individuals and cardiac mitochondrial respiration from different individuals. At the organismal level, oxygen consumption increased in line with warming, and was followed by a return to pre-acclimated levels just after the end of the heat stress. Conversely, cardiac mitochondrial respiration decreased during the heat stress, especially 24 h in, and recovered at the end of the event. Our results suggest that the heat stress was responsible for a metabolic mismatch in the strebers. Indeed, we observed (i) a strong thermodynamic effect without any acclimation process, suggesting that the range of temperatures chosen was not stressful for the fish, and (ii) the establishment of a transitory energy saving process. Our results underline the need for more integrative studies to understand how organisms will adapt to climate change.

**KEY WORDS:** Acute warming, Ectotherms, Metabolic rate, Oxygen consumption, Mitochondrial respiration, Heart

<sup>1</sup>CNRS, ENTPE, Laboratoire d'Écologie des Hydrosystèmes Naturels et Anthropisés (LEHNA) UMR 5023, Université Claude Bernard Lyon 1, Villeurbanne, F-69100, France. <sup>2</sup>INRAE, Aix-Marseille University, UMR RECOVER, 13100 Aix-en-Provence, France. <sup>3</sup>Plateforme Animalerie Conventioennelle et Sauvage Expérimentale de la Doua (ACSED), Fédération de Recherche 3728, Univ. Lyon, Université Claude Bernard Lyon 1, CNRS, ENS-Lyon, INRAE, INSA, VetAgroSup 69622, Villeurbanne, France. <sup>4</sup>Department of Biology, Section for Evolutionary Ecology, Lund University, Sölvegatan 37, SE-223 62 Lund, Sweden. <sup>5</sup>Littoral Environnement et Sociétés (LIENSs), UMR 7266 CNRS - La Rochelle Université, 2 Rue Olympe de Gouges, 17000 La Rochelle, France.

\*These authors contributed equally to this work

‡Author for correspondence (loic.teulier@univ-lyon1.fr)

 J.W., 0009-0005-4485-9049; C.S., 0009-0004-4482-5829; F.-X.D.-M., 0000-0001-7607-8224; D.R., 0000-0002-8865-5428; R.L., 0000-0002-5710-4551; L.R., 0009-0005-2647-0013; A.M.-M., 0000-0001-5264-3989; Y.V., 0000-0003-0572-7199; M.D., 0009-0004-4604-4903; E.T., 0000-0001-5218-9907; L.T., 0000-0001-7779-7634

Received 15 January 2025; Accepted 18 April 2025

## INTRODUCTION

Climate change will increase the frequency and severity of extreme climate events such as storms, hurricanes, floods and heatwaves, which could lead to larger thermal variability (Easterling et al., 2000). The magnitude of the effects of such temperature variations on ectotherms hence depends on the animal's physiological and/or behavioural plasticity (Norin and Metcalfe, 2019). In the context of a rapid temperature increase leading to an acute heat stress, limited metabolic plasticity may lead to the extinction of species that lack the ability to adapt to extreme thermal variations (Cicchino et al., 2024; Seebacher et al., 2015), and particularly during critical phases of their life cycle, such as the spawning period (Béjean, 2019).

When facing stressful conditions, bioenergetics underpin the dynamic nature of physiological plasticity by facilitating the allocation of resources towards acclimation processes, such as maintenance of ion gradients, synthesis of stress-responsive proteins and repair of cellular damage (Jutfelt et al., 2024; Sokolova, 2021). These processes are costly, and their induction leads to an increase of energy expenditure for maintenance. The metabolic rate of an organism has thus become a valuable proxy of its overall health status, including stress levels, growth, reproductive capacities and, ultimately, long-term fitness (Metcalfe et al., 2016; Pettersen and Metcalfe, 2024). Among the different indicators, basal oxygen consumption rate, or standard metabolic rate (SMR) in ectotherms, is the most commonly measured metric corresponding to the minimal energy expenditure mainly associated with the maintenance of vital functions (Chabot et al., 2016a,b; Killen et al., 2021). It is well known that ectothermic species facing acute warming increase their metabolic rate (Fry, 1971; Jutfelt, 2020; Kirby et al., 2020) and a number of studies show that metabolic rate also increases with warm acclimation temperatures in several species (Claireaux et al., 2006, in sea bass, *Dicentrarchus labrax*; Cominassi et al., 2022, in threespine stickleback, *Gasterosteus aculeatus*; Healy and Schulte, 2012, in killifish, *Fundulus heteroclitus*). However, thermal compensation in resting cardiorespiratory functions has been observed in populations acclimated to warm conditions for three decades (Sandblom et al., 2016). This metabolic compensation was also implemented in fish that were food deprived for 60 days during winter (Thoral et al., 2023).

It is crucial to correlate *in vivo* metabolic rate with mitochondrial activity in order to fully understand how organisms respond to environmental fluctuations (Metcalfe et al., 2023; Thoral et al., 2024). Indeed, about 90% of the oxygen is consumed by mitochondria in cells (Brand et al., 1991; Else et al., 2004) in order to produce energy in the form of ATP, through the activity of the electron transport system (ETS) coupled to the activity of ATP synthases. This process, known as oxidative phosphorylation (OXPHOS), is particularly influenced by temperature, which affects mitochondrial coupling, i.e. the amount of ATP produced

per molecule of oxygen consumed, and its maximum capacity (Blier et al., 2014; Chung et al., 2018a; Chung and Schulte, 2020; Rich and Maréchal, 2010). Many studies have shown that an acute increase in assay temperature induces a rise in mitochondrial respiration rates as a result of a  $Q_{10}$  effect (Bouchard and Guderley, 2003; Christen et al., 2018; Iftikar and Hickey, 2013; Pichaud et al., 2017). After the end of a heat stress, one could expect a decline in respiration rates after a few days as acclimation processes could be implemented. Indeed, mitochondrial respiration returns to values similar to those measured before warming, with a decrease in respiration rate a few days after the occurrence of an acute rise in temperature in rainbow trout, *Oncorhynchus mykiss* (Pichaud et al., 2017), and after long acclimation periods in sea bass, *D. labrax* (Voituron et al., 2022b).

The heart emerges as an organ of choice when investigating the effects of temperature variation on animal survival and cellular bioenergetics, because of (i) its continuous aerobic activity, predominantly relying on mitochondrial metabolism (Little et al., 2020); (ii) its critical role in distributing oxygen and nutrients to all body tissues (Little et al., 2020); and (iii) its high thermal sensitivity, making it one of the first organs to fail when fish are exposed to acute high temperatures, alongside the brain (Aslanidi and Kharakoz, 2021; Ern et al., 2023). As mitochondrial function declines, the capacity to supply ATP diminishes. However, ATP requirements increase with rising temperatures, leading to cellular dysfunction if these demands are not met (Hickey et al., 2024). In addition, cardiac mitochondrial thermal sensitivity and plasticity appear to be the primary determinants constraining heart function (Christen et al., 2018; Chung and Schulte, 2020; Gerber et al., 2020; Iftikar and Hickey, 2013; Michaelsen et al., 2021). While the literature extensively explores the effects of high temperatures on fish mitochondria (Blier et al., 2014; Chung et al., 2018b; Chung and Schulte, 2020), few studies have examined mitochondrial flexibility in the heart during an acute heat stress with a rapid temperature increase, a short plateau phase and a rapid return to the initial temperature.

By combining *in vivo* metabolic rate and *in vitro* heart mitochondrial respiration, the main goal of this study was to characterize the metabolic flexibility of an endemic French freshwater fish, the Rhône streber (*Zingel asper*), during a mild heat stress period through a rapid temperature increase from 13°C to 18°C in 5 h and for 5 days. The Rhône streber is a benthic species belonging to the Percidae family, known for its heightened sensitivity to the physio-chemical conditions of its habitat. Its conservation is a significant concern, as it is classified as endangered on the IUCN red list (IUCN Red List of Threatened Species 2025; <https://www.iucnredlist.org/>). Although there is very limited documentation regarding its thermal tolerance, it appears that the streber's reproductive success and growth are highly dependent on environmental temperatures. This raises concerns about the long-term viability of populations in the context of climate change (Béjean, 2019). The range of temperature variation chosen in this study may naturally occur during spring, potentially presenting energetic challenges during the spawning period. We thus compared the experimental group with two control groups: one acclimated at 13°C and another acclimated at 18°C for 6 weeks. We expected that temperature variation would represent a significant transitory energetic challenge for this fish, as temperature appears to be a key driver of the streber's fitness (Béjean, 2019). Moreover, we expected that the experimental group would display an elevated *in vivo* metabolic rate and increased mitochondrial respiration at the onset and during the heat stress. Given the energetic demands imposed by the heat stress, we anticipated delayed returns of these levels to baseline after the decrease in temperature.

## MATERIALS AND METHODS

### Experimental animals and temperature acclimation procedure

Because of their specific status of critically endangered species (Béjean, 2019), Rhône strebers, *Zingel asper* (Linnaeus 1758), were sourced from artificial reproduction in an experimental conservation breeding facility (Museum de Besançon, Citadelle de Besançon, France). Two batches of 4–5 month old fish were successively moved to the animal care facility (ACSED, University Claude Bernard Lyon 1, Lyon, France) in January 2021 ( $n=16$ ) and February 2023 ( $n=76$ ). Therefore, at the beginning of the experiment, fish were between 1 and 3 years old. They were reared in 60 l aquariums filled with filtered, dechlorinated and oxygenated water at 19°C and enriched with plastic plants, gravel and hiding places (PVC tubes), following a standard day:night cycle of 12 h:12 h, and fed once a day with a ration of frozen chironomid larvae (Europrix, France). Six weeks before starting the experiment, fish from the first batch ( $n=16$ ) were acclimated to 18°C, corresponding to the control group 'CT18'. At the same time, fish from the second batch ( $n=76$ ) were progressively acclimated to 13°C (−1°C every 4 h) for 6 weeks, to constitute either the control group 'CT13' or the future experimental groups undergoing the heat stress (HS) and decrease in temperature after the heat stress (DC). It has been shown that age does not influence specific oxygen consumption in adult fish (Fidhiany and Winckler, 1998) and that it has only a small effect on mitochondrial respiration, with a general decrease observed in older individuals (Chouinard-Boisvert et al., 2024). Moreover, mathematical modelling and otolithometry have helped show that there is a correlation between age and body mass in fish (He and Stewart, 2002; Lee et al., 2020), which is one of the key factors influencing metabolism (Hochachka et al., 2003). As oxygen consumption was measured per unit of mass ( $\text{mg O}_2 \text{ h}^{-1} \text{ kg}^{-1}$ ) and as mass was considered during the analysis of mitochondrial respiration data, we made the decision not to randomly assign the first batch to different experimental groups. To avoid any experimental artefact, each group was randomly split into two aquariums 6 days before the experiment. During the whole experiment, the CT13 and CT18 groups were constantly held at 13°C or 18°C, respectively. At day 0, temperature was increased from 13°C to 18°C (+1°C  $\text{h}^{-1}$ ) in the HS aquariums, then maintained at 18°C during 5 consecutive days, and finally decreased from 18°C to 13°C (−1°C  $\text{h}^{-1}$ ) to return to the initial temperature (Fig. 1A). Each aquarium was equipped with a thermostat (ITC-308, Inkbird, Shenzhen, China) for temperature regulation and was either heated with a submersible water heater (75 W, EHEIM) or cooled via a water bath system (TECO TK500 Aquarium Cooler and EHEIM universal 600 pump).

The fish used for cellular bioenergetics were different from the ones used for *in vivo* metabolic rate, except for the fish sampled at the very end after the temperature decrease (these fish came from the *in vivo* experiment). The fish going through the heat stress and decrease periods for *in vivo* metabolic rate will be referred to as the HS group, and those for cellular bioenergetics as the HS and DC groups. All fish were fasted for 24 h before *in vivo* or cellular experiments to control nutritional status.

All the experiments were approved by the Ministère Français de l'Enseignement Supérieur, de la Recherche et de l'Innovation (APAFIS# #28715-2020121714392623 v1).

### Biometry

As a control for good housing conditions, fish body mass and Fulton's index, which is considered as an index of body condition,

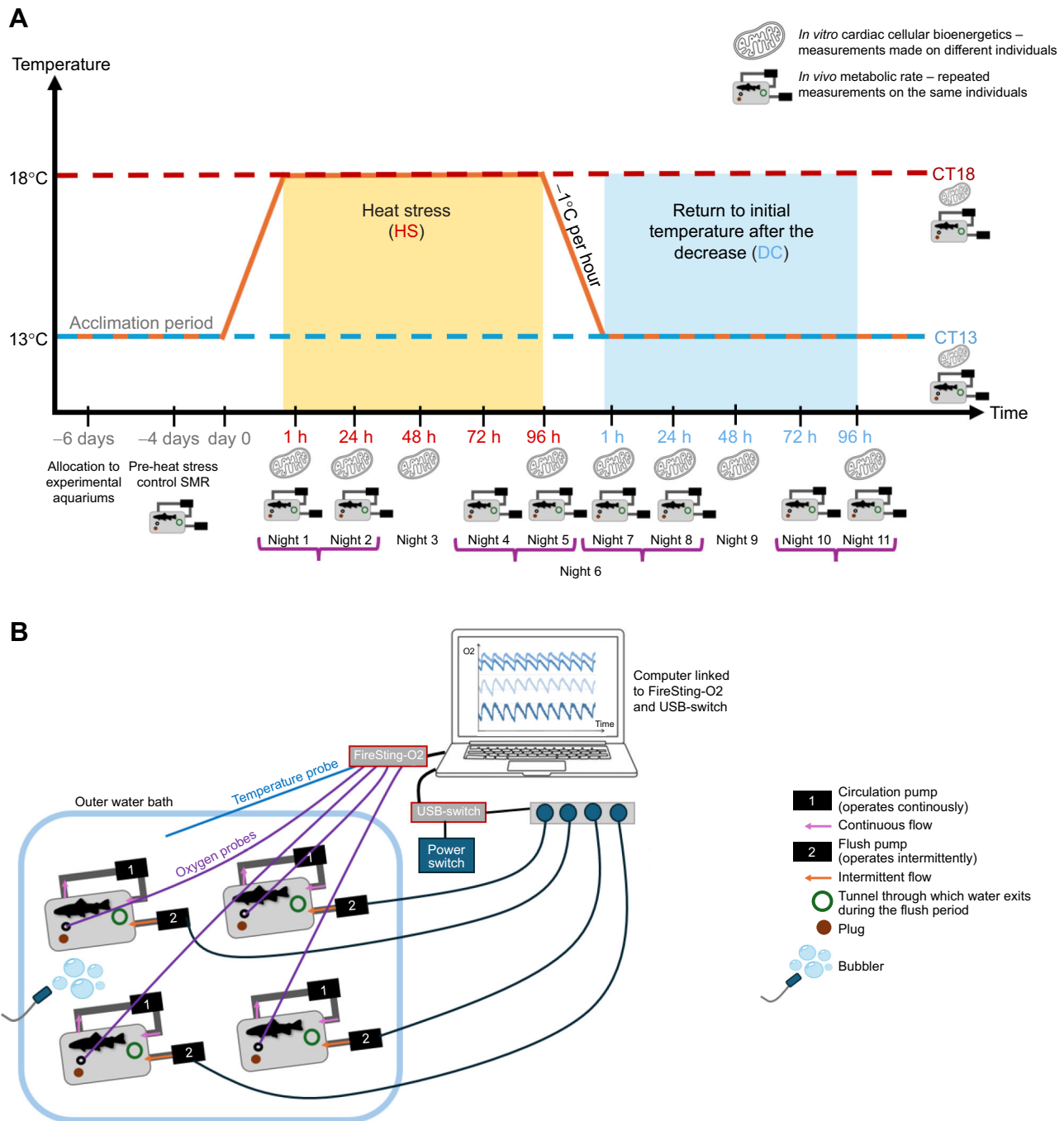


**Fig. 1. Overview of the experimental design and set up for the *in vivo* metabolic rate measurements.** (A) All the Rhône strebers (*Zingel asper*) were allocated to their experimental aquariums 6 days before the beginning of the experiments. Full body respirometry was performed on 16 individuals in total with an interval of 1 week between each run, so on 8 individuals at a time, with 4 controls [2 for control 13°C (CT13) and 2 for control 18°C (CT18)] and 4 experimental individuals (heat stress, HS). The yellow shading represents the heat stress period and the blue shading represents the decrease period. Pre-heat stress control individual standard metabolic rate (SMR) was measured 4 days before the beginning of the experiment over one night. For the rest of the experiment, SMR was measured over two nights (indicated by purple brackets): 1–24 h into the heat stress (nights 1 and 2) then 72–96 h into the heat stress (nights 4 and 5) and then over the same time line after the temperature decrease (nights 7 and 8, then nights 10 and 11). Mitochondrial respiration was measured in control and treated fish 1, 24, 48 and 96 h during the heat stress (HS1, HS24, HS48 and HS96) and then over the same time line after the decrease in temperature (DC1, DC24, DC48, DC96). (B) Measurement of oxygen consumption ( $\dot{M}_{O_2}$ ). For respirometry details, please refer to Materials and Methods.

were collected (Table 1). Fulton's index was calculated as follows (Nash et al., 2006):

$$\text{Fulton's index} = \frac{\text{Body mass}}{\text{Size}^3} \times 100, \quad (1)$$

where body mass is in grams and size is in centimetres.

#### ***In vivo* metabolic rate**

Whole-organism respirometry was performed on 16 individuals in total (4 CT13, 4 CT18 and 8 HS). To allow repeated measurements on the same individuals, these fish were tagged just behind the dorsal fin with Visible Implant Elastomere Tags for individual recognition (Rácz et al., 2021) 6 days before the beginning of the

**Table 1. Body mass and body condition (Fulton's index) among the different treatment groups**

Group	Body mass (g)	Fulton's index
CT13	3.16±0.30 <sup>a</sup>	0.60±0.01 <sup>a</sup>
CT18	5.77±0.51 <sup>b</sup>	0.62±0.02 <sup>a,b</sup>
HS1	3.81±0.29 <sup>a,c</sup>	0.62±0.02 <sup>a,b</sup>
HS24	3.59±0.20 <sup>a,c</sup>	0.61±0.02 <sup>a,b</sup>
HS48	3.66±0.22 <sup>a,c</sup>	0.62±0.01 <sup>a,b</sup>
HS96	3.67±0.23 <sup>a,c</sup>	0.62±0.02 <sup>a,b</sup>
DC1	3.13±0.28 <sup>a,c</sup>	0.69±0.02 <sup>a,b</sup>
DC24	3.95±0.29 <sup>a,c</sup>	0.70±0.02 <sup>b</sup>
DC48	4.84±0.41 <sup>b,c</sup>	0.69±0.01 <sup>b</sup>
DC96	3.72±0.53 <sup>a,c</sup>	0.61±0.04 <sup>a,b</sup>

Body mass and body length were measured after the fish were euthanized for mitochondrial respiration and are represented as means±s.e.m. Controls at 13 and 18°C: CT13  $n=10$ , CT18  $n=10$ ; heat stress at 1, 24, 48 and 96 h: HS1  $n=10$ , HS24  $n=8$ , HS48  $n=8$ , HS96  $n=8$ ; temperature decrease at 1, 24, 48 and 96 h: DC1  $n=7$ , DC24  $n=8$ , DC48  $n=8$ , DC96  $n=4$ . Different letters indicate a significant difference between the experimental groups with  $P<0.05$  according to *post hoc* tests corrected with Tukey's method.

experiment. Nine measurements of oxygen consumption ( $\dot{M}_{O_2}$ ) were repeated on each individual with an interval of 1 week between each run (see details below). The experiment was performed on 8 individuals at a time: 4 controls (2 CT13 and 2 CT18) and 4 experimental HS individuals (Fig. 1).

To measure  $\dot{M}_{O_2}$ , fish were individually placed in a polyethylene respirometer (0.65 l; 15.1×10.8×6.9 cm, Lock-n-lock Co, Seoul, South Korea) immersed in an outer water bath. Water was constantly regulated at 13°C and 18°C for CT13 ( $n=4$ ) and CT18 ( $n=4$ ) groups, respectively, and at 13°C or 18°C depending on the time line of the heat stress for the experimental HS group ( $n=8$ ). The temperature of the outer water bath was regulated by a water bath system (TECO TK500 Aquarium Cooler and EHEIM universal 600 pump) and it was surrounded by black and opaque plastic bags to prevent any visual disturbance to the fish. Each respirometer was connected to a circulation pump (MaxiJet Micro, Aquarium Systems) that continuously pumped water within the respirometer, and a flush pump (EHEIM compactON 300) that operated intermittently through a PC-controlled power switch (USB-Switch, Cleware Engineering Solutions) (Fig. 1B). This allowed alternation of water renewal (3 min), wait (2 min) and measurement periods (5 min) using the Aquaresp software (V3.0, <https://zenodo.org/records/2584015>).

This 'intermittent-stop flow' protocol enabled  $\dot{M}_{O_2}$  (in  $\text{mgO}_2 \text{ h}^{-1} \text{ kg}^{-1}$ ) to be measured over a long period without hypoxia (Svendsen et al., 2016). Oxygen concentration was continuously recorded using optodes (Robust oxygen probes, Pyrosience) connected to an oxygen meter (FireSting-O2, Pyrosience). Ambient pressure and water temperature were also continuously recorded each second. All data were collected with the OxygenLogger software (Pyrosience). Background respiration was measured in empty respirometers for 3 whole cycles (30 min) before the fish were put in the respirometers and after they were taken out. When necessary, mean background respiration for each temperature was subtracted from all the fish's oxygen consumption values. The SMR was taken as the average of the 10% lowest oxygen consumption values measured each night the fish were in the respirometers (Chabot et al., 2016a,b; Thoral et al., 2022a).

SMR was measured over 9 different time points along the experimental procedure for each individual (Fig. 1). First, control SMR was measured over one night (from 18:00 h to 08:30 h) 4 days before the beginning of the heat stress at 13°C for the CT13 and the HS groups, and at 18°C for the CT18 group. Then, on day 0, the HS

fish acclimated at 13°C were placed in a respirometry chamber during the early afternoon to undergo the progressive increase in temperature up to 18°C (+1°C per hour). SMR was then measured overnight for the first hour after reaching 18°C ('1 h' heat stress point during night 1) and the next night to measure the '24 h' heat stress point (night 2). Thereafter, SMR was similarly measured after 72 h (night 4) and 96 h (night 5) of heat stress, and 1, 24, 72 and 96 h after being returned to 13°C (nights 7, 8, 10 and 11). At days 3, 6 and 9, fish were removed from the respirometers and placed back in their respective acclimation tanks to be re-fed (Fig. 1). CT13 and CT18 fish followed the same protocol as for the HS fish but were constantly measured at 13°C or at 18°C, respectively.

### Cellular bioenergetics

In order to describe the effect of an acute heat stress on heart cell bioenergetics, cardiac mitochondrial respiration rate was measured in the HS group after reaching 18°C for 1 h (HS1,  $n=8$ ), 24 h (HS24,  $n=8$ ), 48 h (HS48,  $n=8$ ) and 96 h (HS96,  $n=8$ ), and after returning to 13°C for 1 h (DC1,  $n=7$ ), 24 h (DC24,  $n=8$ ), 48 h (DC48,  $n=8$ ) and 96 h (DC96,  $n=4$ ). CT13 ( $n=10$ ) and CT18 ( $n=10$ ) mitochondrial measurements were assayed following the same time line to control for a potential effect of time (Fig. 1). Sample sizes vary because of technical issues that occurred during the experiment.

Fish were euthanized with 150  $\text{mg l}^{-1}$  of buffered MS-222 in oxygenated water, followed by decapitation. Then, fish were weighed, and their sex was defined by dissection and visual determination of gonads. The heart was removed, weighed and immediately placed in an ice-cold MiR05 buffer (0.5  $\text{mmol l}^{-1}$  EGTA, 3  $\text{mmol l}^{-1}$   $\text{MgCl}_2 \cdot 6\text{H}_2\text{O}$ , 60  $\text{mmol l}^{-1}$  potassium lactobionate, 20  $\text{mmol l}^{-1}$  taurine, 10  $\text{mmol l}^{-1}$   $\text{KH}_2\text{PO}_4$ , 20  $\text{mmol l}^{-1}$  Hepes, 110  $\text{mmol l}^{-1}$  sucrose and 1  $\text{g l}^{-1}$  fatty acid-free bovine serum albumin, pH 7.1 at 15°C). The heart was homogenized in 500  $\mu\text{l}$  MiR05 using a Potter–Elvehjem homogenizer (10 passages). The total mean ( $\pm$ s.e.m.) heart mass was 3.79±1.16 mg.

An aliquot of the homogenate (150  $\mu\text{l}$ ) was added to a 2 ml glass cell filled with MiR05 buffer. Mitochondrial respiration was measured using high-resolution respirometers (Oroboros O2k, Oroboros® Instruments, Innsbruck, Austria), thermostatically controlled at either 13°C or 18°C (all fish were measured at both temperatures). Mitochondrial respiration rate of fish hearts was measured following a protocol of sequential injection of substrates, inhibitors and uncouplers (SUIT protocol) adapted from Thoral et al. (2022b) and Teulier et al. (2019). Briefly, a combination of complex I (CI) respiratory substrates (5  $\text{mmol l}^{-1}$  pyruvate/2.5  $\text{mmol l}^{-1}$  malate/10  $\text{mmol l}^{-1}$  glutamate) was injected to obtain the basal non-phosphorylating respiration rate associated with proton leak activity (LEAK CI), followed by the addition of ADP (1  $\text{mmol l}^{-1}$ ) to initiate the phosphorylation respiration rate as it activates ATP synthase. Cytochrome *c* (10  $\mu\text{mol l}^{-1}$ ) was then added to test the integrity of the outer mitochondrial membrane. The resulting respiration was considered as the CI-supported oxidative phosphorylation respiration (OXPHOS CI). Then, succinate (5  $\text{mmol l}^{-1}$ ), as a complex II (CII) substrate, was used to assess complexes I+II-supported oxidative phosphorylation respiration (OXPHOS CI+CII), followed by the addition of oligomycin (2.5  $\mu\text{mol l}^{-1}$ ), an inhibitor of ATP synthase, to obtain LEAK respiration with CI+II activated (LEAK CI+CII). Antimycin A (5  $\mu\text{mol l}^{-1}$ ) was then injected to inhibit mitochondrial respiration to estimate non-mitochondrial residual respiration (ROX respiration). This residual oxygen consumption was removed from all the other respiration rates. This was followed by injections of ascorbate (2.5  $\text{mmol l}^{-1}$ ), tetramethyl-*p*-phenylenediamine

(TMPD,  $0.5 \text{ mmol l}^{-1}$ ) and  $2 \mu\text{mol l}^{-1}$  carbonyl cyanide-*p*-trifluoro-methoxyphenyl hydrazine (FCCP) to fully activate the cytochrome *c* oxidase (COX), an indicator of total mitochondrial oxidative capacity. Finally, sodium azide ( $20 \text{ mmol l}^{-1}$ ) was injected to inhibit COX activity and assess the auto-oxidation of ascorbate/TMPD substrates. COX activity was calculated by subtracting the azide-insensitive oxygen consumption from the ascorbate/TMPD/FCCP-induced fully uncoupled oxygen consumption of COX.

We also calculated a cellular aerobic scope (cAS), an index of the aerobic capacity of the mitochondria for CI (OXPHOS CI–LEAK CI) and CI+CII (OXPHOS CI+CII–LEAK CI+CII), and the respiratory control ratio (RCR) for CI (OXPHOS CI/LEAK CI) and CI+CII (OXPHOS CI+CII/LEAK CI+CII).

### Statistical analysis

All data were analysed with R version 4.4.2 (<http://www.R-project.org/>). For *in vivo* metabolic rate, the ‘*lmer*’ function from the *lme4* package (Bates et al., 2015) was employed to integrate linear mixed models using backwards stepwise selection. Treatment and time were used as fixed effects, and individual as a random effect to consider repeated measures designed for SMR. Normality and heteroscedasticity assumptions were checked for model residuals with the *qqplot()* and *qqnorm()* functions, and log transformations were applied when needed to meet normality assumptions. Consequently, the data shown in the Results section were log-transformed to meet the assumptions and to reduce variability. First, to analyse SMR, both control groups (CT13 and CT18) were tested against each other over the whole experiment to see whether there were any differences between both groups. Then, each period was studied separately: first the pre-heat stress period, then the heat stress period and then the post-decrease period. For each period, CT13 and CT18 groups were compared with the HS group and among each other. Effect size indexes for metabolic parameters were calculated with Cohen’s *d* coefficients with the ‘*cohen.d*’ function from the *effsize* package.

We analyzed mitochondrial respiration rates using linear mixed models with treatment, assay temperature ( $13^\circ\text{C}$  or  $18^\circ\text{C}$ ) and body mass as fixed effects, and individual as a random effect because each individual was assayed at both temperatures. Then, we aimed

to mitigate the influence of temperature by normalizing the respiration rates by COX respiration as COX activity is very sensitive to temperature and an indicator of mitochondrial content (Larsen et al., 2012). We analyzed mitochondrial respiration rates normalized by COX respiration using linear models, incorporating treatment and body mass as fixed effects. Firstly, a linear model was employed to see whether there were any differences between both control groups (CT13 and CT18) and the same was done for the heat stress groups (HS1, HS24, HS48 and HS96) on one side and for the decrease groups (DC1, DC24, DC48 and DC96) on the other. If there were no inter-group differences, the pooled groups (CT groups CT13+CT18 pooled together; HS groups HS1+HS24+HS48+HS96 pooled together; and DC groups DC1+DC24+DC48+DC96 pooled together) were then tested against each other to see whether there were any differences between them. Secondly, all the separate groups (CT13, CT18, HS1, HS24, HS48, HS96, DC1, DC24, DC48, DC96) were tested for differences between each other in a general model. This method was also used to analyse body mass and Fulton index. Normality and heteroscedasticity assumptions were checked for model residuals with the *qqplot()* and *qqnorm()* functions, and log transformations were applied when needed to meet normality assumptions. As log transformations did not change the outcome compared with the raw data, we kept raw data for the analysis. Effect size indexes for mitochondrial parameters were estimated with the ‘*eff\_size*’ function from the *emmeans* package because they were calculated from the fitted models and allowed the adjustment for covariates such as body mass and assay temperature through the model.

For each method, stepwise model selection was performed using  $\chi^2$  tests, followed by Tukey’s *post hoc* pairwise comparisons when required from the *multcomp* package. *P*-values less than 0.05 were considered as significant; sample sizes varied slightly between parameters because of missing data due to technical issues.

## RESULTS

### *In vivo* metabolic rate

Our results did not show any difference between the regression slopes of the CT13 and the CT18 groups ( $\chi^2_1=3.46$ ,  $P=0.063$ ; Fig. 2). However, there was an effect of thermal treatment, with a higher SMR among the CT18 group at  $18^\circ\text{C}$  (scaled estimate

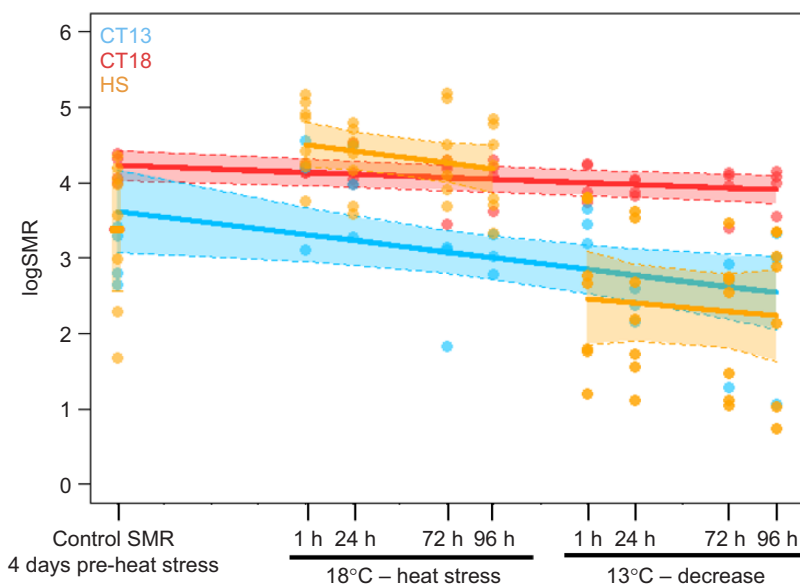


**Fig. 2. SMR of the different groups during the experimental period.** SMR values ( $\text{mg O}_2 \text{ h}^{-1} \text{ kg}^{-1}$ ) were log transformed to reduce the data’s variance. The blue and red lines represent the CT13 and CT18 groups, respectively. The orange lines represent the HS group. Circles represent individual values. SMR was measured repeatedly on the same individuals. Control SMR was measured 4 days before the beginning of the heat stress in all groups. During the heat stress period, SMR was measured at 1, 24, 72 and 96 h, and after the temperature decrease, it was measured at 1, 24, 72 and 96 h as well.

$\beta=1.36$ , 95% confidence interval CI=[0.97; 1.76],  $\chi^2_1=9.48$ ,  $P=0.002$ ), and an additive effect of time (scaled estimate  $\beta=-0.27$ , 95% CI=[-0.44; -0.10],  $\chi^2_1=16.9$ ,  $P<0.001$ ), with a decrease in SMR over the whole experiment. Among the HS group, SMR changed between the different phases (i.e. before, during and after the heat stress;  $\chi^2_2=68.81$ ,  $P<0.001$ ). During the pre-heat stress measurement, there was no difference between the HS and the CT13 groups (scaled estimate  $\beta=0.78$ , 95% CI=[-0.54; 2.10],  $F_{1,10}=1.75$ ,  $P=0.22$ ), which is consistent as the two groups were held at the same acclimation temperature. During the heat stress, there was an effect of treatment ( $\chi^2_2=12.25$ ,  $P=0.002$ ), as the SMR of the HS group was higher than that of the CT13 group (*post hoc* test:  $\beta=1.49$ , 95% CI=[0.60; 2.37],  $P<0.001$ ) but not different from that of the CT18 group (*post hoc* test:  $\beta=0.39$ , 95% CI=[-0.41; 1.19],  $P=0.49$ ). Thus, the rise in temperature from 13°C to 18°C led to a significant increase in the SMR of the HS group compared with the values obtained in the same individuals during the pre-heat stress measurement. Moreover, 1 h into the heat stress, the HS group exhibited a tendency for an extra metabolic cost compared with the CT18 group, with a higher SMR (Cohen's  $d=-0.90$ , 95% CI=[-2.32; 0.53]). After the end of the heat stress, there was still an effect of thermal treatment ( $\chi^2_2=21.37$ ,  $P<0.001$ ) with a higher SMR in the HS group compared with the CT18 group (*post hoc* test: scaled estimate  $\beta=-1.53$ , 95% CI=[-2.26; -0.81],  $P<0.001$ ). However, no significant difference was measured between the SMR of the HS and CT13 groups (*post hoc* test:  $\beta=-0.28$ , 95% CI=[-1.07; 0.51];  $P=0.69$ ). However, the SMR of the HS group tended to be lower than that of the CT13 group 1 h following the temperature decrease (Cohen's  $d=0.67$ , 95% CI=[-0.96; 2.30]).

### Mitochondrial respiration

As expected, the linear mixed model indicated that the mitochondrial parameters LEAK and OXPHOS with CI and CI+II-linked substrates, cAS and COX activity were, overall, significantly higher when measured at 18°C than at 13°C, regardless of the group (Fig. 3; Fig. S1 and Tables S1, S2 and S3). RCR values were not significantly affected by assay temperature (Fig. 3D; Fig. S1C and Table S2). All results considered, the model also indicated that the heat stress elicited significant alteration in OXPHOS respiration with both CI-linked (Fig. 3A; linear mixed model:  $F_{9,69,84}=2.43$ ,  $P=0.02$ ) and CI+II-linked substrates (Fig. S1A). On the whole, these OXPHOS rates were significantly lower in the HS than in the DC and CT groups (linear mixed models: HS–DC:  $F_{1,58,27}=5.72$ ,  $P=0.02$ , and HS–CT:  $F_{1,51,08}=7.97$ ,  $P<0.01$ ). In contrast, respiration rates of the CT and DC groups did not differ significantly (linear mixed model:  $F_{1,44}=0.80$ ,  $P=0.37$ ). More specifically, the HS24 group had significantly lower respiration rates than the CT18 group ( $P=0.03$ , not shown in Fig. 3A). Among all individual groups, some other differences tended also to be significant, regardless of assay temperature, and globally even though  $P>0.2$ , they had a very high effect size. Hence, the HS24 group tended to have lower respiration than the CT13 group ( $P=0.16$ , effect size=1.46, 95% CI: [0.37, 2.55]), the HS1 group ( $P=0.27$ , effect size=1.36, 95% CI: [0.26, 2.45]), the DC1 group ( $P=0.29$ , effect size=1.45, 95% CI: [0.26, 2.63]), the DC48 group ( $P=0.17$ , effect size=1.60, 95% CI: [0.40, 2.79]) and the DC96 group ( $P=0.15$ , effect size=1.91, 95% CI: [0.51, 3.31]). Moreover, the HS48 group tended to have lower respiration rates than the CT13 group ( $P=0.44$ , effect size=1.20, 95% CI: [0.11, 2.29]), the CT18 group ( $P=0.10$ , effect size=1.77, 95% CI: [0.54, 3.01]), the DC48 group ( $P=0.41$ , effect size=1.33, 95% CI: [0.14, 2.51]) and the DC96 group ( $P=0.34$ , effect size=1.64, 95% CI: [0.25, 3.04]).

LEAK CI respiration rates did not follow the same pattern as OXPHOS respiration rates (Fig. 3B), but the model was significant overall (linear mixed model:  $F_{9,69,99}=3.09$ ,  $P<0.01$ ). All data considered, the CT group had higher LEAK respiration than the HS and DC groups (linear mixed model: CT–HS:  $F_{1,50,80}=13.44$ ,  $P<0.001$  and CT–DC:  $F_{1,44}=5.74$ ,  $P=0.02$ ), while LEAK did not differ between the HS and DC groups (linear mixed model:  $F_{1,57,76}=1.67$ ,  $P=0.10$ ; Fig. 3B). The same pattern applied for LEAK CI+II respiration (Fig. S1B). Regardless of assay temperature, the *post hoc* test highlights that the CT18 group had significantly higher LEAK respiration than the HS1 ( $P<0.01$ ), HS24 ( $P=0.03$ ), DC24 ( $P=0.03$ ) and DC48 groups ( $P=0.03$ ) (not shown in Fig. 3B). It had a strong tendency to be so compared with the HS48 group ( $P=0.11$ , effect size=2.25, 95% CI: [0.67, 3.83]) and the HS96 group ( $P=0.22$ , effect size=2.02, 95% CI: [0.44, 3.60]). LEAK respiration rates of the HS1 group also tended to be lower than those of the CT13 group ( $P=0.38$ , effect size=1.52, 95% CI: [0.19, 2.85]) and the DC1 group ( $P=0.35$ , effect size=1.71, 95% CI: [0.24, 3.18]).

cAS CI (Fig. 3C) followed the same pattern as the OXPHOS CI respiration rates and showed an effect of treatment group (linear mixed model:  $F_{9,69,87}=2.09$ ,  $P=0.04$ ). On the whole, cAS CI was significantly lower in the HS groups than in the DC and CT groups (linear mixed models: HS–DC:  $F_{1,58,33}=5.06$ ,  $P=0.03$ ; HS–CT:  $F_{1,51,13}=5.42$ ,  $P=0.02$ ). In contrast, cAS of the CT and DC groups did not differ significantly (linear mixed model:  $F_{1,44}=0.21$ ,  $P=0.65$ ). cAS CI+II followed the same pattern as cAS of CI alone (Table S2A,B).

RCR CI (Fig. 3D) showed an effect of treatment group (linear mixed model:  $F_{9,69,71}=2.04$ ,  $P=0.05$ ). When applying a *post hoc* test, the HS1 group had a higher ratio than the HS48 group ( $P=0.04$ ) and this group also tended to have a higher ratio than the HS24 group ( $P=0.10$ , effect size=1.85, 95% CI: [0.55, 3.14]), regardless of assay temperature. However, regardless of assay temperature and despite some differences among the HS groups (between the HS1 and HS48 groups), there were no differences between CT, HS and DC groups (linear mixed model: CT–HS:  $F_{1,51,11}=0.11$ ,  $P=0.91$ ; CT–DC:  $F_{1,44}=1.21$ ,  $P=0.28$ ; DC–HS:  $F_{1,58,23}=0.72$ ,  $P=0.40$ ). RCR CI+II followed the same pattern as RCR of CI alone (Fig. S1C).

Mitochondrial oxidative capacity (Fig. 3E), measured as maximal COX activity, showed an effect of treatment group (linear mixed model:  $F_{9,67,62}=3.07$ ,  $P<0.01$ ). When applying a *post hoc* test, the HS1 group had higher respiration rates than the DC24 and HS48 groups (both  $P<0.01$ ). However, regardless of assay temperature and despite some differences among the HS groups (between the HS1 and HS48 groups), there were no differences between the CT, HS and DC groups (linear mixed model: CT–HS:  $F_{1,48,37}=0.12$ ,  $P=0.73$ ; CT–DC:  $F_{1,43,65}=1.79$ ,  $P=0.19$ ; DC–HS:  $F_{1,54,79}=0.85$ ,  $P=0.36$ ).

In order to separate the  $Q_{10}$  effect from the direct consequence of heat stresses on fish mitochondrial respiration rates, all of the rates were divided by COX respiration rates, assuming that the whole ETS and COX have similar  $Q_{10}$  values (Fig. 4; Table S4). This approach allowed a more eco-physiological comparison of mitochondrial respiration between respiration measured at 13°C (CT13 and DC groups) and that measured during the heat stress at 18°C (CT18 and HS groups). Overall, OXPHOS CI respiration rates in the HS groups were lower than those in the CT groups (linear mixed model:  $F_{1,49}=5.44$ ,  $P=0.02$ ) and DC groups (linear mixed model:  $F_{1,55}=10.13$ ,  $P<0.01$ ; Fig. 4A). OXPHOS respiration rates of the CT and DC groups did not significantly differ from each other (linear mixed model:  $F_{1,43}=0.05$ ,  $P=0.82$ ). When applying a *post hoc* test, the HS24 group exhibited a lower OXPHOS respiration than the CT18 and DC48 groups (linear mixed model: respectively,

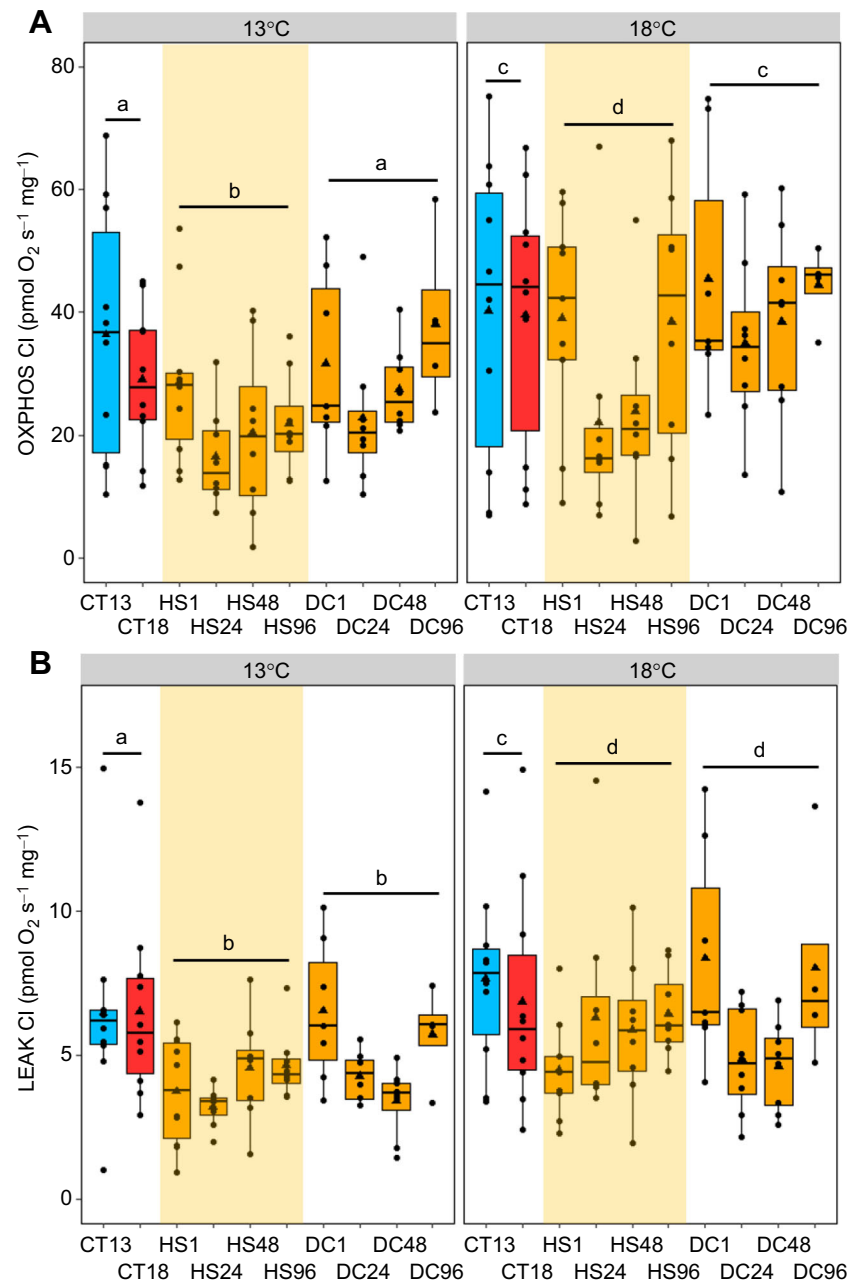


Fig. 3. Continued on next page.

$P=0.04$  and  $P=0.02$ , not shown in Fig. 4A), and tended to be so compared with the CT13 group ( $P=0.13$ , effect size=1.36, 95% CI: [0.38, 2.35]), the DC1 group ( $P=0.35$ , effect size=1.29, 95% CI: [0.18, 2.40]), the DC24 group ( $P=0.26$ , effect size=1.28, 95% CI: [0.25, 2.30]) and the DC96 group ( $P=0.12$ , effect size=1.78, 95% CI: [0.52, 3.04]).

For normalized LEAK CI respiration (Fig. 4B), the model was not significant overall (linear mixed model:  $F_{9,67}=1.66$ ,  $P=0.11$ ). However, the HS1 group tended to have lower respiration rates than the CT13 group ( $P=0.19$ , effect size=1.30, 95% CI: [0.31, 2.29]) and the HS48 group ( $P=0.07$ , effect size=-1.57, 95% CI: [-2.16, -0.54]).

## DISCUSSION

This study investigated the metabolic consequences of an acute heat stress at the organismal and cellular levels in Rhône strebers. At the

whole-organism level, fish facing the heat stress exhibited a fully reversible cycle of increase/decrease in oxygen consumption, certainly due to a thermodynamic effect of temperature. At the cellular level, heart bioenergetics followed an interesting reversible and resilient pattern, with a transient down-regulated activity of mitochondrial OXPPOS respiration, especially 24 h into the heat stress, which returned to pre-acclimation levels after 96 h, at the onset of the temperature decrease.

### A fully reversible metabolic rate during and after the heat stress

#### A thermodynamic effect

As observed in many studies performed in aquatic ectotherms (Clarke and Fraser, 2004; Fry, 1971; Jutfelt, 2020; Kirby et al., 2020), we found that *in vivo* SMR closely aligned with the

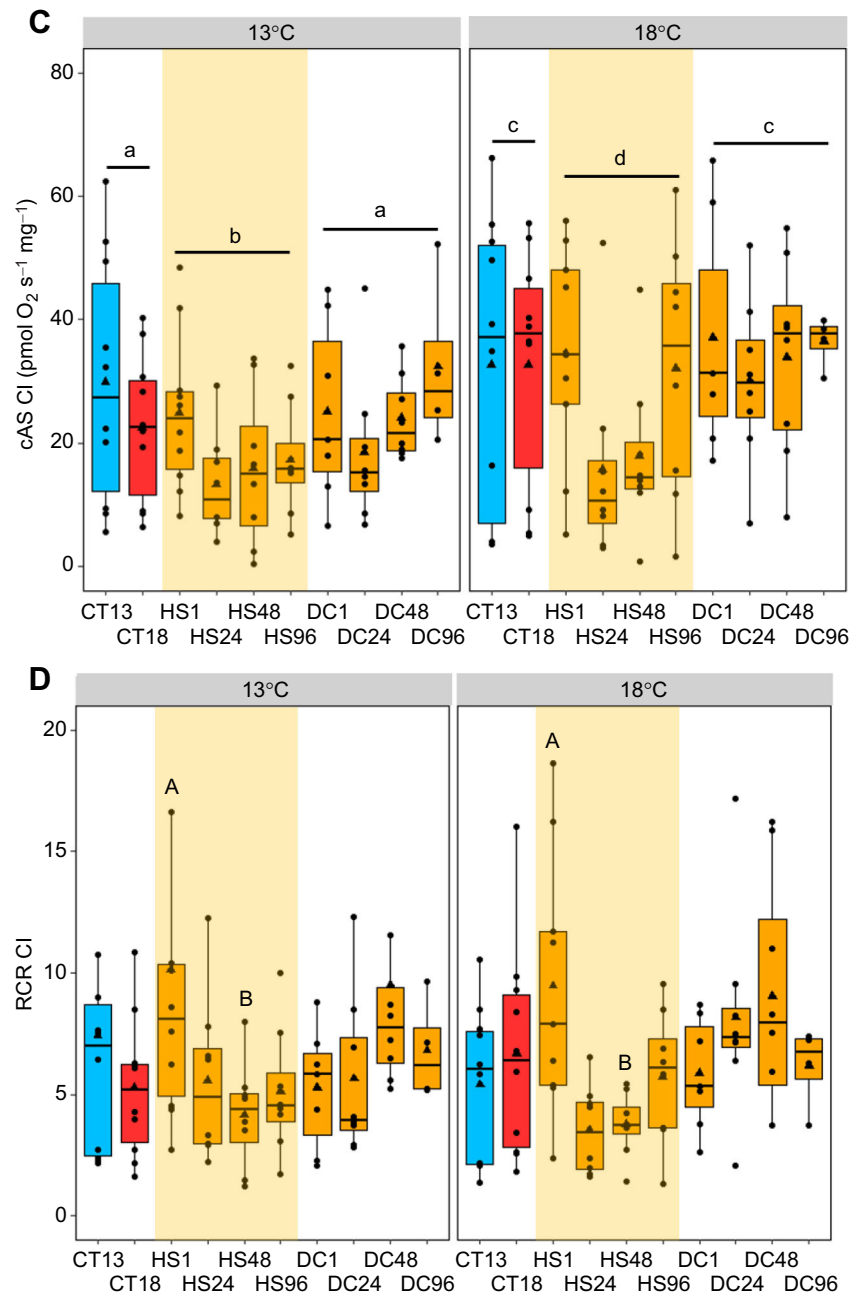
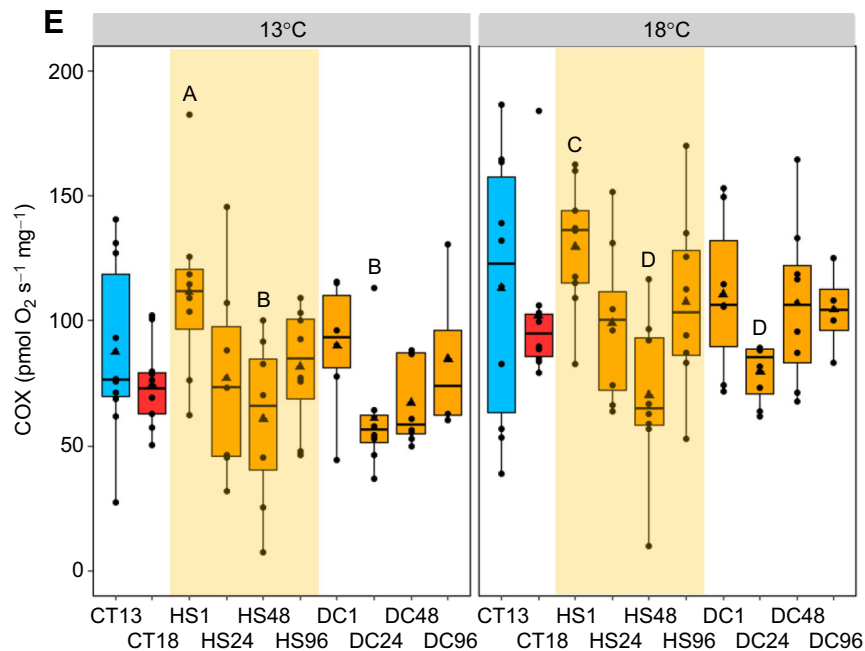


Fig. 3. Continued on next page.

temperature pattern induced by the heat stress, with an increase, a plateau and a decrease, ultimately returning to pre-acclimation levels. These results align with recent experiments on the Australasian snapper (*Chrysothys auratus*) and the golden grey mullet (*Chelon auratus*) facing marine heatwaves, as defined in the literature (Hobday et al., 2016), which revealed similar metabolic patterns during heat stress conditions (Bowering et al., 2023; Grimmelpont et al., 2023). The Australasian snapper exhibited an elevated SMR 1 day after the temperature was increased from 21°C to 25°C, maintaining this elevated state for 30 days (Bowering et al., 2023). Similarly, golden grey mullet increased their SMR during the heat stress (from 20°C to 25°C), reaching levels comparable to those of control fish maintained at 25°C (Grimmelpont et al., 2023).

Interestingly, SMR returned to pre-acclimation levels either directly 1 h after the temperature decrease in the Rhône streber (present study), or 7 days after the end of a heatwave in the golden grey mullet (Grimmelpont et al., 2023). The latter observation in grey mullet could be partly explained by a higher oxygen debt accumulated during heat stress, showing a higher cost to acclimate to 25°C. In contrast, in our study, the SMR of strebers returned immediately to levels similar to those obtained before the heat stress, suggesting no metabolic cost following the 5 day heat stress in this species. Given that the strebers' vulnerability could be mainly associated with thermal risk (Béjean, 2019), we were expecting a significant extra cost with an increased SMR at the beginning of the heat stress. Indeed, the increase in SMR in the HS group 1 h after the rise in temperature did not differ significantly from the SMR of the



**Fig. 3. Mitochondrial respiration rates among the different experimental groups according to assay temperature.** Different respiration rates are represented and all values are in  $\text{pmol O}_2 \text{ s}^{-1} \text{ mg}^{-1}$  heart mass: complex I-supported oxidative phosphorylation (OXPHOS CI; A), respiration associated with proton leak activity (LEAK CI; B), cellular aerobic scope (cAS) CI (calculated as  $\text{OXPHOS CI} - \text{LEAK CI}$ ; C), respiratory control ratio (RCR) CI (calculated as  $\text{OXPHOS CI} / \text{LEAK CI}$ ; D) and cytochrome *c* oxidase (COX) activity (E). Different colours indicate different treatment groups: the CT13 group is in blue, the CT18 group is in red and the HS1, HS24, HS48, HS96, DC1, DC24, DC48 and DC96 groups are all in orange. The circles represent individual values. The triangles on the boxplots represent the mean and the boxplots show the median, upper and lower quartiles and  $1.5 \times$  the interquartile range. The yellow shading represents the interval of the heat stress. Control groups were assayed throughout the whole experiment. For the sake of visibility, the scales are not the same for each graph.  $n=4-10$  for each group. In A–C, different lowercase letters indicate a significant difference between the groups evaluated, specifically among the CT, HS and DC groups, with  $P < 0.05$  according to *post hoc* tests corrected with Tukey's method. For differences between individual groups, refer to Results. In D and E, different capital letters indicate a significant difference between individual groups, with  $P < 0.05$  according to *post hoc* tests corrected with Tukey's method.

CT18 fish (Cohen's  $d=0.84$ , Fig. 2). The absence of an increased  $\dot{M}\text{O}_2$  during the acute phase of temperature decrease suggests no oxygen debt, which could mean that the increase in temperature from  $13^\circ\text{C}$  to  $18^\circ\text{C}$  did not represent a real energetic challenge for the Rhône strebers. Even if  $18^\circ\text{C}$  is far lower than the highest temperature recorded in natural French rivers around the strebers' natural habitat, the rapid increase of  $+5^\circ\text{C}$  ( $1^\circ\text{C h}^{-1}$ ) from  $13^\circ\text{C}$  to  $18^\circ\text{C}$  represents nonetheless the warmest range of temperatures undergone by fish during their artificial life cycle (Béjean, 2019). Moreover, this range of acute temperature increase may naturally happen during early spring, which constitutes a critical period for fish in terms of energetic constraints due to reproduction. Currently, we lack comprehensive insight into whether  $18^\circ\text{C}$  constitutes a stressful temperature for these fish, as there is very little information on their thermal tolerance. Indeed, critical thermal maximum ( $\text{CT}_{\text{max}}$ ) trials have never been conducted on this species, and we do not possess information regarding their aerobic scope either. Here, metabolic variations seem to be dictated by temperature only with a thermodynamic  $Q_{10}$  effect (Clarke and Fraser, 2004; Fry, 1971). This phenomenon is known as 'non-adaptive' or 'passive plasticity', which defines acute sensitivity as opposed to 'active plasticity', which defines a specific organismal response (Gotthard et al., 1995; Schulte et al., 2011). Thus, in the present study, the perfect fit between temperature patterns and metabolic rate, with similar levels reached between the HS and CT18 fish during the heat stress, suggests a strong thermodynamic effect without any acclimation process that could become deleterious during warmer

heat stresses. In other words, the Rhône strebers seemed to show no evidence of active plasticity during this period of heat stress.

#### Metabolic rates remain high in fish chronically exposed to high temperature: a limited ability to adapt or a no-stress condition?

In the case of chronic warming, the literature has shown that thermal compensation in warm-adapted fish populations (Sandblom et al., 2016, in yellow perch, *Perca flavescens*) and in food-deprived fish (Thoral et al., 2023, in European sardine, *Sardina pilchardus*) does exist. However, in several species, acclimation to higher temperatures does not always reduce metabolic rate (Claireaux et al., 2006, in sea bass, *Dicentrarchus labrax*; Cominassi et al., 2022, in threespine stickleback, *Gasterosteus aculeatus*; Healy and Schulte, 2012, in killifish, *Fundulus heteroclitus*). In the present study, fish chronically exposed to  $18^\circ\text{C}$  exhibited a higher SMR compared with that of fish at  $13^\circ\text{C}$ , even after 2 months of thermal exposure, indicating a limited ability to acclimate. Such elevation of SMR may suggest the need for additional energy to support maintenance functions in fish, which could reduce fitness and performance (Chabot et al., 2016a,b). However, in the case of *ad libitum* food availability such as in our experimental conditions, it is not surprising that fish SMR remained high, allowing individuals to maintain function, without needing to lower their energy expenditure (Auer et al., 2015, 2016). However, further investigations are needed to fully understand the potential interaction between thermal acclimation and nutritional status and its putative role in the disappearance of this species, and to better

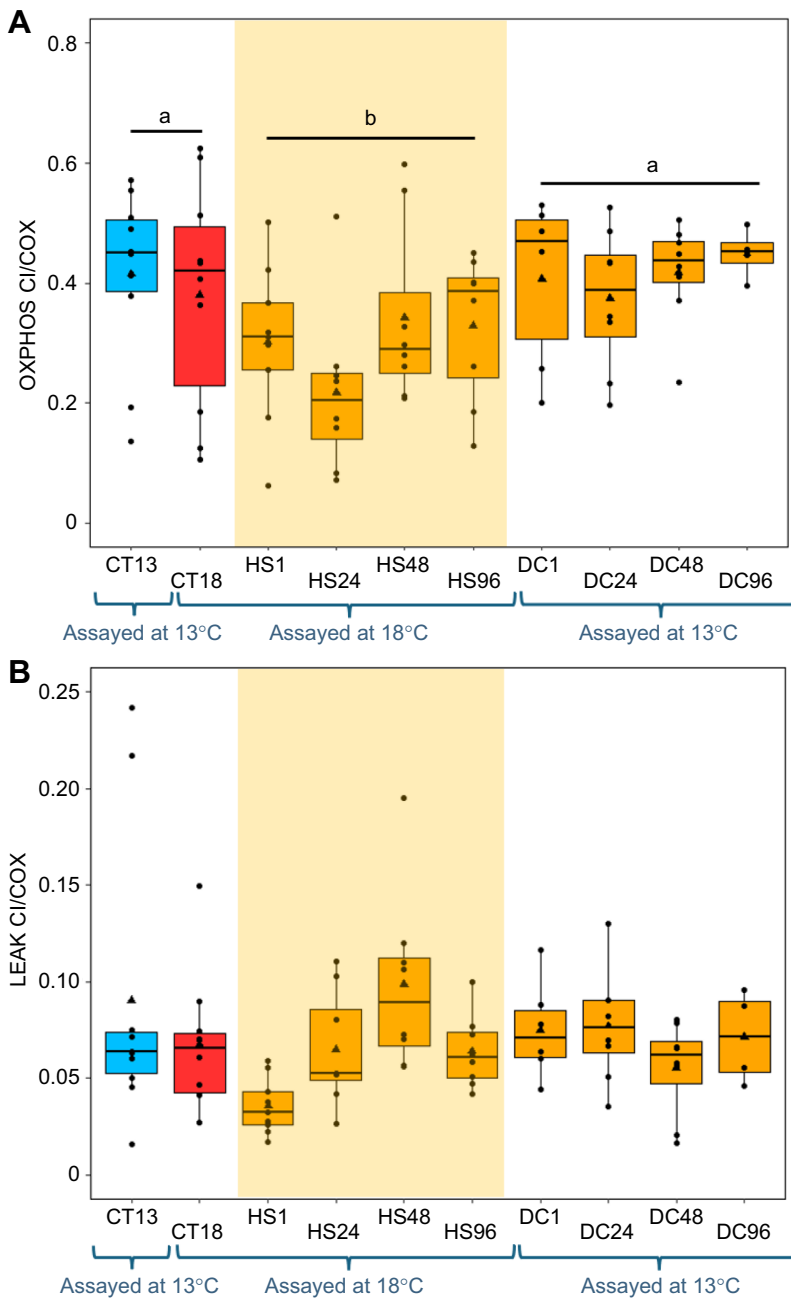


**Fig. 4. Mitochondrial respiration rates normalized by COX respiration among the different experimental groups and depending on assay temperature.** Different respiration rates are represented: OXPHOS CI (A) and LEAK CI (B). Respiration for each group is shown assayed at the temperature at which the fish were sampled. This means that the CT13 group is shown assayed at 13°C, the CT18 group at 18°C, the HS1, HS24, HS48 and HS96 groups at 18°C and the DC1, DC24, DC48 and DC96 groups at 13°C. Different colours indicate different treatment groups: the CT13 group is in blue, the CT18 group is in red and the HS1, HS24, HS48, HS96, DC1, DC24, DC48 and DC96 groups are all in orange. The circles represent individual values. The triangles on the boxplots represent the mean and the boxplots show the median, upper and lower quartiles and 1.5× the interquartile range. The yellow shading represents the interval of the heat stress. For the sake of visibility, the scales are not the same for each graph.  $n=4-10$  for each group. In A, different lowercase letters indicate a significant difference between the groups evaluated, specifically among the CT, HS and DC groups, with  $P<0.05$  according to *post hoc* tests corrected with Tukey's method. For differences between individual groups, refer to Results.

understand the consequences for aquatic fauna of ongoing anthropogenic global change (Queiros et al., 2024).

#### Mitochondrial bioenergetics in the warm Mitochondrial oxidative phosphorylation is reduced during heat stress

When assessing mitochondrial metabolism, an acute increase in assay temperature is well known to induce a rise in mitochondrial respiration rates up to a threshold, beyond which electron transport is impaired and oxygen flux decreases (Blier et al., 2014; Bouchard and Guderley, 2003; Christen et al., 2018; Chung et al., 2017; Hilton et al., 2010; Kraffe et al., 2007; Pichaud et al., 2017). As expected, in our study, we also found an increase in cardiac mitochondrial oxygen consumption at warm temperatures (18°C versus 13°C). Given the results obtained at the *in vivo* level, showing no evidence of active plasticity during the heat stress

(probably via the establishment of cellular and molecular compensatory mechanisms), we were expecting no major dysfunction of mitochondrial metabolism with the rise in temperature. Surprisingly, and contrary to our hypothesis, we found that OXPHOS and LEAK respiration in the heart were decreased during the heat stress and especially after 24 h. More specifically, OXPHOS respiration rates were 40% lower on average in HS fish compared with CT13 and CT18 fish, whereas LEAK rates only exhibited a moderate 15% decrease. These differential respiratory changes explain the decrease in cAS as well as in RCR, which could in turn indicate a proportionate decrease in the rate of ATP synthesis.

This metabolic mismatch induced by the heat stress, with an increase in SMR and a decrease in cardiac mitochondrial activity, suggests a major metabolic stress at the cellular level. There are several possible reasons for a mitochondrial dysfunction in the

heart. For example, there could be an impairment in membrane permeability and/or an increased thermal sensitivity of the ETS complexes (Seebacher et al., 2010). Indeed, elevated temperatures are known to increase proton permeability in mitochondrial membranes (Chamberlin, 2004; Chung and Schulte, 2015; Dufour et al., 1996), leading to a decrease in mitochondrial coupling efficiency (Brooks et al., 1971; Iftikar and Hickey, 2013; Roussel et al., 2023; Roussel and Voituron, 2020; Salin et al., 2012), which can ultimately lead to a decrease in ATP synthesis (Iftikar and Hickey, 2013; Salin et al., 2015). However, this scenario does not seem to be at play in the present study, as maximal proton leak activity (i.e. LEAK CI+CI2) was only marginally affected in the heart of fish going through the heat stress (Figs 3B and 4B; Fig. S1B). Instead, there was a marked decrease in OXPHOS respiration, in particular associated with CI activity, which triggered a sudden decline in RCR from 24 to 48 h into the heatwave, indicating that mitochondrial coupling would be at stake and ATP synthesis compromised during the stress. CI has been reported to be sensitive to high temperature in insects and fish (Gerber et al., 2020; Jørgensen et al., 2021; Menail et al., 2022; Pichaud et al., 2019). In particular, differential thermal sensitivity of ETS complexes has been reported in cardiac mitochondria of fish (Chung and Schulte, 2015; Gerber et al., 2020; Pichaud et al., 2017), with high temperatures affecting the activity of CI and CIII but not that of CII and COX (Lemieux et al., 2010). However, the sharp decrease in CI-supported respiration at high temperature in insects can be compensated for by the oxidation of other alternative substrates, such as proline, glycerol 3-phosphate and in particular succinate, which allows the maintenance of mitochondrial ATP synthesis (Jørgensen et al., 2021; Menail et al., 2022; Roussel et al., 2023). Yet, contrary to insects, failure of CI-supported OXPHOS was not compensated for by oxidation of succinate in cardiac mitochondria of rainbow trout (*O. mykiss*) (Michaelsen et al., 2021) and the Rhône streber (present study).

#### Fish heart mitochondria: acute heat stress versus thermal acclimation

The negative impact of acute warming on mitochondrial bioenergetics 24 h into heat stress was transient, as OXPHOS respiration increased progressively during the next 48 h. Interestingly, this result is in line with the findings of a study investigating the effect of heat stress in Australasian snappers (*C. auratus*), which showed a transient decrease in cardiac OXPHOS rates 1 day into the heat stress, returning to its pre-acclimation levels after 10 days of heat stress (Bowering et al., 2023). Another study, conducted on rainbow trout (Pichaud et al., 2017), showed that cardiac mitochondrial oxygen consumption rates increased slightly during an acute warming, which can be explained by a thermodynamic action of temperature on mitochondrial processes, and then decreased 1 day later when the temperature was still high. The present study clearly suggests that the alteration of OXPHOS activity was transient, occurring 24 h after the heat stress started and returning to its initial level 96 h into the heat stress, and during the decrease in temperature. Similarly, the recovery from two successive heat stresses or one long period of heat stress did not result in variations of mitochondrial parameters in the red muscle of zebrafish (*Danio rerio*) (Thoral et al., 2022b). Altogether, these data indicate that a prolonged exposure to elevated temperatures, or an extended recovery period after a warm event, allows organisms to mitigate the effects of a heat stress.

Fish naturally exposed to warm temperatures have a greater ability to maintain mitochondrial oxidative phosphorylation activity when environmental temperature increases (Hilton et al., 2010). Several

studies clearly indicate that thermal acclimation can allow fish to reset their mitochondrial bioenergetics and survive in warmer habitats (Bouchard and Guderley, 2003; Pichaud et al., 2017; Voituron et al., 2022b). After acclimation to warmer environments, mitochondrial bioenergetics can return to their pre-acclimation level by a reduction in their respiration rates (Pichaud et al., 2017; Voituron et al., 2022b). In our study, it appears that this process was probably established within the CT18 group, as their respiration rates aligned with those of the CT13 group, regardless of assay temperature (Figs 3 and 4; Fig. S1). Nevertheless, acclimation is a process that takes time to be implemented and often requires cellular mechanisms such as the synthesis of new proteins and membranes, which typically need several weeks to stabilize (Bouchard and Guderley, 2003; Voituron et al., 2022a). In the present study, the alteration of cardiac mitochondrial OXPHOS activity was restored in a few days during the heat stress, and so prior to the onset of the decrease in temperature. In the absence of compensation by the oxidation of alternative substrates (i.e. succinate), this mitochondrial flexibility would involve other fast cellular processes, such as the removal of dysfunctional mitochondria and/or rapid synthesis of heat shock proteins (Pichaud et al., 2017). This highlights a great phenotypic flexibility of mitochondrial bioenergetics, which may confer a buffering role to mitochondria, allowing them to rapidly endure acute energetic challenges. The observed ‘buffering’ in cardiac mitochondrial respiration rates could also be related to other mechanisms set up to save energy and maintain homeostasis during heat stress. For example, maintenance of reaction rates, protein structure and electrical excitability, and at a larger scale, maintenance of organ function, especially neural and somatic muscle function (Ern et al., 2023). A significant portion of the existing literature on mitochondrial recovery following stressful events primarily addresses human health issues such as ischemia–reperfusion and sepsis (Di Lisa and Bernardi, 1998; Singer, 2007). When considering mitochondrial recovery after stressful climatic events, it can be anticipated that the restoration to baseline levels is influenced by both the severity of the stress and the degree of pre-acclimatization that the organism experienced prior to the stress. Further investigations are needed to study the metabolic responses at different times of the recovery phase after a stress, and to explain such fast adjustments of cardiac mitochondrial function in our case.

#### Conclusion and perspectives

Our findings show that a moderate heat stress in Rhône strebers resulted in a transient metabolic mismatch with a thermodynamic increase in whole-organism energy demand on one side (‘passive plasticity’) and a transient alteration in mitochondrial energy-producing mechanisms on the other (‘active plasticity’). Hence, the present study highlights the ability of an endangered fish species to cope with a rapid warming, exhibiting a dramatic but fully reversible impact on mitochondrial metabolism. Given that the vulnerability of the strebers may primarily be related to thermal risk (Béjean, 2019), it is worth asking whether the Rhône strebers can cope with, and survive, several successive or longer period of heat stress, especially during spawning periods.

Connecting whole-body metabolism with mitochondrial function remains of great interest to gain an integrative view of an organism’s response to high temperatures (McKenzie et al., 2021; Metcalfe et al., 2023). In the context of an increasingly variable environment and as performance decreases from its peak level during warming phases, animals must be capable of physiological plasticity to face climate change and to survive. Even though more and more research

is being conducted on the effects of global change on fish physiology and on the ecology of fisheries (Ern et al., 2023; Huey and Kingsolver, 2019; Jutfelt et al., 2024; Little et al., 2020), some dark areas remain. We thus require more integrative studies that establish connections between cellular bioenergetics across different organs, and the overall functioning of the body, to better understand the machinery of physiological plasticity during heat stress (Casagrande et al., 2023; Metcalfe et al., 2023; Salin et al., 2015; Thorall et al., 2024).

#### Acknowledgements

We are grateful to the PNA apron du Rhône, Mickaël Béjean (Citadelle de Besançon, France), for providing the fish and his expertise in streber rearing, to Claire Saraux and Josefa Bleu for helping with the statistical analyses, and to Anthony Maire for the interesting discussions that helped us write this paper.

#### Competing interests

The authors declare no competing or financial interests.

#### Author contributions

Conceptualization: J.W., C.S., E.T., L.T.; Data curation: J.W., C.S., D.R., J.L.G., R.L., L.R., E.T., L.T.; Formal analysis: J.W., C.S., F.-X.D.-M., E.T.; Funding acquisition: F.-X.D.-M., M.D., L.T.; Investigation: J.W., C.S., D.R., J.L.G., R.L., L.R., E.T., L.T.; Methodology: J.W., C.S., F.-X.D.-M., D.R., L.G., L.R., E.T., L.T.; Project administration: L.T.; Supervision: E.T., L.T.; Validation: J.W., C.S., F.-X.D.-M., D.R., J.L.G., R.L., L.G., A.C., L.A., C.B., L.R., A.M.-M., Y.V., M.D., E.T., L.T.; Writing – original draft: J.W., C.S.; Writing – review & editing: J.W., C.S., F.-X.D.-M., D.R., J.L.G., R.L., L.G., A.C., L.A., C.B., L.R., A.M.-M., Y.V., M.D., E.T., L.T.

#### Funding

This work was supported by Électricité de France (EDF) as part of the project 'CARAPATE', the Heatwaves project and the BiodiverSâone project of the Agence de l'Eau Rhône-Méditerranée-Corse (AE-RMC). J.W.'s PhD is funded by the 'CARAPATE' project and C.S.'s PhD is funded by the BioverSaône project.

#### Data and resource availability

The code and data used for this project are available from Zenodo: <https://doi.org/10.5281/zenodo.15166583>

#### ECR Spotlight

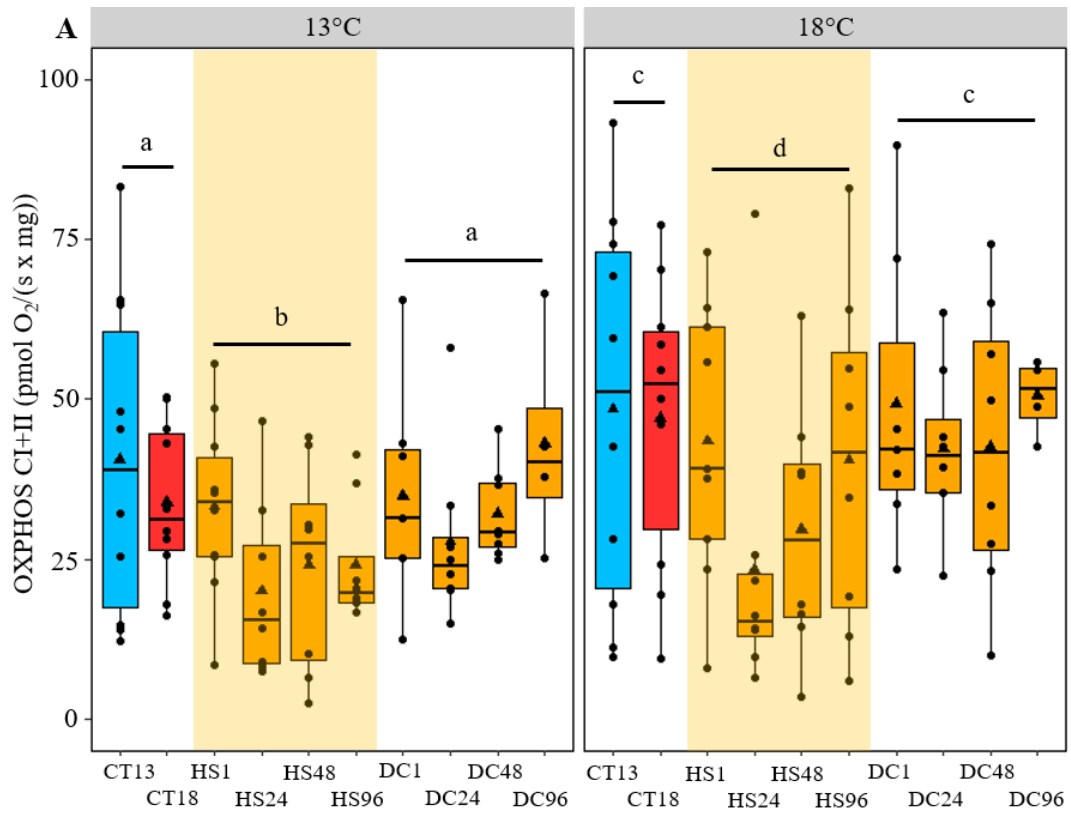
This article has an associated ECR Spotlight interview with Julia Watson and Chloé Souques.

#### References

- Aslanidi, K. B. and Kharakoz, D. P. (2021). Limits of temperature adaptation and thermopreferendum. *Cell Biosci.* **11**, 69. doi:10.1186/s13578-021-00574-9
- Auer, S. K., Salin, K., Rudolf, A. M., Anderson, G. J. and Metcalfe, N. B. (2015). The optimal combination of standard metabolic rate and aerobic scope for somatic growth depends on food availability. *Funct. Ecol.* **29**, 479-486. doi:10.1111/1365-2435.12396
- Auer, S. K., Salin, K., Rudolf, A. M., Anderson, G. J. and Metcalfe, N. B. (2016). Differential effects of food availability on minimum and maximum rates of metabolism. *Biol. Lett.* **12**, 20160586. doi:10.1098/rsbl.2016.0586
- Bates, D., Mächler, M., Bolker, B. and Walker, S. (2015). Fitting linear mixed-effects models using lme4. *J. Stat. Softw.* **67**, 1-48. doi:10.18637/jss.v067.i01
- Béjean, M. (2019). Reproduction of *Zingel asper* (Linnaeus, 1758) in controlled conditions: an assessment of the experiences realized since 2005 at the Besançon Natural History Museum. *Cybiurn* **43**, 17-32. doi:10.26028/CYBIUM/2019-431-002
- Blier, P. U., Lemieux, H. and Pichaud, N. (2014). Holding our breath in our modern world: Will mitochondria keep the pace with climate changes? *Can. J. Zool.* **92**, 591-601. doi:10.1139/cjz-2013-0183
- Bouchard, P. and Guderley, H. (2003). Time course of the response of mitochondria from oxidative muscle during thermal acclimation of rainbow trout, *Oncorhynchus mykiss*. *J. Exp. Biol.* **206**, 3455-3465. doi:10.1242/jeb.00578
- Bowering, L. R., McArley, T. J., Devaux, J. B. L., Hickey, A. J. R. and Herbert, N. A. (2023). Metabolic resilience of the Australasian snapper (*Chrysophrys auratus*) to marine heatwaves and hypoxia. *Front. Physiol.* **14**, 1215442. doi:10.3389/fphys.2023.1215442
- Brand, M. D., Couture, P., Else, P. L., Withers, K. W. and Hulbert, A. J. (1991). Evolution of energy metabolism. Proton permeability of the inner membrane of liver mitochondria is greater in a mammal than in a reptile. *Biochem. J.* **275**, 81-86. doi:10.1042/bj2750081
- Brooks, G. A., Hittelman, K. J., Faulkner, J. A. and Beyer, R. E. (1971). Temperature, skeletal muscle mitochondrial functions, and oxygen debt. *Am. J. Physiol. Legacy Content* **220**, 1053-1059. doi:10.1152/ajplegacy.1971.220.4.1053
- Casagrande, S., Dzialo, M., Trost, L., Malkoc, K., Sadowska, E. T., Hau, M., Pierce, B., McWilliams, S. and Bauchinger, U. (2023). Mitochondrial metabolism in blood more reliably predicts whole-animal energy needs compared to other tissues. *iScience* **26**, 108321. doi:10.1016/j.isci.2023.108321
- Chabot, D., McKenzie, D. J. and Craig, J. F. (2016a). Metabolic rate in fishes: definitions, methods and significance for conservation physiology. *J. Fish Biol.* **88**, 1-9. doi:10.1111/jfb.12873
- Chabot, D., Steffensen, J. F. and Farrell, A. P. (2016b). The determination of standard metabolic rate in fishes. *J. Fish Biol.* **88**, 81-121. doi:10.1111/jfb.12845
- Chamberlin, M. E. (2004). Top-down control analysis of the effect of temperature on ectotherm oxidative phosphorylation. *Am. J. Physiol. Regul. Integr. Comp. Physiol.* **287**, R794-R800. doi:10.1152/ajpregu.00240.2004
- Chouinard-Boisvert, S., Ghinter, L., St-Pierre, A., Mortz, M., Desrosiers, V., Dufresne, F., Tardif, J.-C., Huard, J., Sirois, P., Fortin, S. et al. (2024). Mitochondrial functions and fatty acid profiles in fish heart: an insight into physiological limitations linked to thermal tolerance and age. *J. Exp. Biol.* **227**, jeb247502. doi:10.1242/jeb.247502
- Christen, F., Desrosiers, V., Dupont-Cyr, B. A., Vandenberg, G. W., Le François, N. R., Tardif, J.-C., Dufresne, F., Lamarre, S. G. and Blier, P. U. (2018). Thermal tolerance and thermal sensitivity of heart mitochondria: mitochondrial integrity and ROS production. *Free Radic. Biol. Med.* **116**, 11-18. doi:10.1016/j.freeradbiomed.2017.12.037
- Chung, D. J. and Schulte, P. M. (2015). Mechanisms and costs of mitochondrial thermal acclimation in a eurythermal killifish (*Fundulus heteroclitus*). *J. Exp. Biol.* **218**, 1621-1631. doi:10.1242/jeb.120444
- Chung, D. J. and Schulte, P. M. (2020). Mitochondria and the thermal limits of ectotherms. *J. Exp. Biol.* **223**, jeb227801. doi:10.1242/jeb.227801
- Chung, D. J., Bryant, H. J. and Schulte, P. M. (2017). Thermal acclimation and subspecies-specific effects on heart and brain mitochondrial performance in a eurythermal teleost (*Fundulus heteroclitus*). *J. Exp. Biol.* **220**, 1459-1471. doi:10.1242/jeb.151217
- Chung, D. J., Healy, T. M., McKenzie, J. L., Chicco, A. J., Sparagna, G. C. and Schulte, P. M. (2018a). Mitochondria, temperature, and the pace of life. *Integr. Comp. Biol.* **58**, 578-590. doi:10.1093/icb/icy013
- Chung, D. J., Sparagna, G. C., Chicco, A. J. and Schulte, P. M. (2018b). Patterns of mitochondrial membrane remodeling parallel functional adaptations to thermal stress. *J. Exp. Biol.* **221**, jeb174458. doi:10.1242/jeb.174458
- Cicchino, A. S., Ghalambor, C. K., Forester, B. R., Dunham, J. D. and Funk, W. C. (2024). Greater plasticity in CTmax with increased climate variability among populations of tailed frogs. *Proc. R. Soc. B* **291**, 20241628. doi:10.1098/rspb.2024.1628
- Claireaux, G., Couturier, C. and Groison, A.-L. (2006). Effect of temperature on maximum swimming speed and cost of transport in juvenile European sea bass (*Dicentrarchus labrax*). *J. Exp. Biol.* **209**, 3420-3428. doi:10.1242/jeb.02346
- Clarke, A. and Fraser, K. P. P. (2004). Why does metabolism scale with temperature? *Funct. Ecol.* **18**, 243-251. doi:10.1111/j.0269-8463.2004.00841.x
- Cominassi, L., Ressel, K. N., Brooking, A. A., Marbacher, P., Ransdell-Green, E. C. and O'Brien, K. M. (2022). Metabolic rate increases with acclimation temperature and is associated with mitochondrial function in some tissues of threespine stickleback. *J. Exp. Biol.* **225**, jeb244659. doi:10.1242/jeb.244659
- Di Lisa, F. and Bernardi, P. (1998). Mitochondrial function as a determinant of recovery or death in cell response to injury. In *Bioenergetics of the Cell: Quantitative Aspects* (ed. V. A. Saks, R. Ventura-Clapier, X. Leverve, A. Rossi and M. Rigoulet), pp. 379-391. Springer US. doi:10.1007/978-1-4615-5653-4\_25
- Dufour, S., Rousse, N., Canioni, P. and Diolez, P. (1996). Top-down control analysis of temperature effect on oxidative phosphorylation. *Biochem. J.* **314**, 743-751. doi:10.1042/bj3140743
- Easterling, D. R., Meehl, G. A., Parmesan, C., Changnon, S. A., Karl, T. R. and Mearns, L. O. (2000). Climate extremes: observations, modeling, and impacts. *Science* **289**, 2068-2074. doi:10.1126/science.289.5487.2068
- Else, P. L., Brand, M. D., Turner, N. and Hulbert, A. J. (2004). Respiration rate of hepatocytes varies with body mass in birds. *J. Exp. Biol.* **207**, 2305-2311. doi:10.1242/jeb.01017
- Ern, R., Andreassen, A. H. and Jutfelt, F. (2023). Physiological mechanisms of acute upper thermal tolerance in fish. *Physiology* **38**, 141-158. doi:10.1152/physiol.00027.2022
- Fidhiany, L. and Winckler, K. (1998). Influence of body mass, age, and maturation on specific oxygen consumption in a freshwater Cichlid Fish, *Cichlasoma nigrofasciatum* (Günther, 1869). *Comp. Biochem. Physiol. A Mol. Integr. Physiol.* **119**, 613-619. doi:10.1016/S1095-6433(97)00474-1
- Fry, F. E. J. (1971). The effect of environmental factors on the physiology of fish. In *Fish Physiology* (ed. W. S. Hoar and D. J. Randall), Vol. 6, pp. 1-98. Elsevier. doi:10.1016/S1546-5098(08)60146-6
- Gerber, L., Clow, K. A., Mark, F. C. and Gamperl, A. K. (2020). Improved mitochondrial function in salmon (*Salmo salar*) following high temperature acclimation suggests that there are cracks in the proverbial 'ceiling'. *Sci. Rep.* **10**, 21636. doi:10.1038/s41598-020-78519-4

- Gotthard, K., Nylin, S. and Nylin, S. (1995). Adaptive plasticity and plasticity as an adaptation: a selective review of plasticity in animal morphology and life history. *Oikos* **74**, 3. doi:10.2307/3545669
- Grimmelpont, M., Milinkovitch, T., Dubillot, E. and Lefrançois, C. (2023). Individual aerobic performance and anaerobic compensation in a temperate fish during a simulated marine heatwave. *Sci. Total Environ.* **863**, 160844. doi:10.1016/j.scitotenv.2022.160844
- He, J. X. and Stewart, D. J. (2002). A stage-explicit expression of the von Bertalanffy growth model for understanding age at first reproduction of Great Lakes fishes. *Can. J. Fish. Aquat. Sci.* **59**, 250-261. doi:10.1139/f02-008
- Healy, T. M. and Schulte, P. M. (2012). Thermal acclimation is not necessary to maintain a wide thermal breadth of Aerobic scope in the common Killifish (*Fundulus heteroclitus*). *Physiol. Biochem. Zool.* **85**, 107-119. doi:10.1086/664584
- Hickey, A. J. R., Harford, A. R., Blier, P. U. and Devaux, J. B. (2024). What causes cardiac mitochondrial failure at high environmental temperatures? *J. Exp. Biol.* **227**, jeb247432. doi:10.1242/jeb.247432
- Hilton, Z., Clements, K. D. and Hickey, A. J. R. (2010). Temperature sensitivity of cardiac mitochondria in intertidal and subtidal triplefin fishes. *J. Comp. Physiol. B* **180**, 979-990. doi:10.1007/s00360-010-0477-7
- Hobday, A. J., Alexander, L. V., Perkins, S. E., Smale, D. A., Straub, S. C., Oliver, E. C. J., Benthuyzen, J. A., Burrows, M. T., Donat, M. G., Feng, M. et al. (2016). A hierarchical approach to defining marine heatwaves. *Prog. Oceanogr.* **141**, 227-238. doi:10.1016/j.pcean.2015.12.014
- Hochachka, P. W., Darveau, C.-A., Andrews, R. D. and Suarez, R. K. (2003). Allometric cascade: a model for resolving body mass effects on metabolism. *Comp. Biochem. Physiol. A Mol. Integr. Physiol.* **134**, 675-691. doi:10.1016/S1095-6433(02)00364-1
- Huey, R. B. and Kingsolver, J. G. (2019). Climate warming, resource availability, and the metabolic meltdown of ectotherms. *Am. Nat.* **194**, E140-E150. doi:10.1086/705679
- Iftikar, F. I. and Hickey, A. J. R. (2013). Do mitochondria limit hot fish hearts? Understanding the role of mitochondrial function with heat stress in *Notolabrus celidotus*. *PLoS ONE* **8**, e64120. doi:10.1371/journal.pone.0064120
- Jørgensen, L. B., Overgaard, J., Hunter-Manseau, F. and Pichaud, N. (2021). Dramatic changes in mitochondrial substrate use at critically high temperatures: a comparative study using *Drosophila*. *J. Exp. Biol.* **224**, jeb240960. doi:10.1242/jeb.240960
- Jutfelt, F. (2020). Metabolic adaptation to warm water in fish. *Funct. Ecol.* **34**, 1138-1141. doi:10.1111/1365-2435.13558
- Jutfelt, F., Ern, R., Leeuwis, R. H. J. and Clark, T. D. (2024). Effects of climate warming. In *Reference Module in Life Sciences* (ed. S. L. Alderman and T. E. Gillis), p. B978032390801600183X. Elsevier. doi:10.1016/B978-0-323-90801-6.00183-X
- Killen, S. S., Christensen, E. A. F., Cortese, D., Závorka, L., Norin, T., Cotgrove, L., Crespel, A., Munson, A., Nati, J. J. H., Papatheodoulou, M. et al. (2021). Guidelines for reporting methods to estimate metabolic rates by aquatic intermittent-flow respirometry. *J. Exp. Biol.* **224**, jeb242522. doi:10.1242/jeb.242522
- Kirby, A. R., Crossley, D. A. and Mager, E. M. (2020). The metabolism and swimming performance of sheepshead minnows (*Cyprinodon variegatus*) following thermal acclimation or acute thermal exposure. *J. Comp. Physiol. B* **190**, 557-568. doi:10.1007/s00360-020-01293-2
- Kraffe, E., Marty, Y. and Guderley, H. (2007). Changes in mitochondrial oxidative capacities during thermal acclimation of rainbow trout *Oncorhynchus mykiss*: Roles of membrane proteins, phospholipids and their fatty acid compositions. *J. Exp. Biol.* **210**, 149-165. doi:10.1242/jeb.02628
- Larsen, S., Nielsen, J., Hansen, C. N., Nielsen, L. B., Wibrand, F., Stride, N., Schroder, H. D., Boushel, R., Helge, J. W., Dela, F. et al. (2012). Biomarkers of mitochondrial content in skeletal muscle of healthy young human subjects. *J. Physiol.* **590**, 3349-3360. doi:10.1113/jphysiol.2012.230185
- Lee, L., Atkinson, D., Hirst, A. G. and Cornell, S. J. (2020). A new framework for growth curve fitting based on the von Bertalanffy growth function. *Sci. Rep.* **10**, 7953. doi:10.1038/s41598-020-64839-y
- Lemieux, H., Tardif, J.-C., Dutil, J.-D. and Blier, P. U. (2010). Thermal sensitivity of cardiac mitochondrial metabolism in an ectothermic species from a cold environment, Atlantic wolffish (*Anarhichas lupus*). *J. Exp. Mar. Biol. Ecol.* **384**, 113-118. doi:10.1016/j.jembe.2009.12.007
- Little, A. G., Loughland, I. and Seebacher, F. (2020). What do warming waters mean for fish physiology and fisheries? *J. Fish Biol.* **97**, 328-340. doi:10.1111/jfb.14402
- McKenzie, D. J., Geffroy, B. and Farrell, A. P. (2021). Effects of global warming on fishes and fisheries. *J. Fish Biol.* **98**, 1489-1492. doi:10.1111/jfb.14762
- Menail, H. A., Cormier, S. B., Ben Youssef, M., Jørgensen, L. B., Vickruck, J. L., Morin, P., Boudreau, L. H. and Pichaud, N. (2022). Flexible thermal sensitivity of mitochondrial oxygen consumption and substrate oxidation in flying insect species. *Front. Physiol.* **13**, 897174. doi:10.3389/fphys.2022.897174
- Metcalfe, N. B., Van Leeuwen, T. E. and Killen, S. S. (2016). Does individual variation in metabolic phenotype predict fish behaviour and performance? *J. Fish Biol.* **88**, 298-321. doi:10.1111/jfb.12699
- Metcalfe, N. B., Bellman, J., Bize, P., Blier, P. U., Crespel, A., Dawson, N. J., Dunn, R. E., Halsey, L. G., Hood, W. R., Hopkins, M. et al. (2023). Solving the conundrum of intra-specific variation in metabolic rate: a multidisciplinary conceptual and methodological toolkit: New technical developments are opening the door to an understanding of why metabolic rate varies among individual animals of a species. *BioEssays* **45**, 2300026. doi:10.1002/bies.202300026
- Michaelsen, J., Fago, A. and Bundgaard, A. (2021). High temperature impairs mitochondrial function in rainbow trout cardiac mitochondria. *J. Exp. Biol.* **224**, jeb242382. doi:10.1242/jeb.242382
- Nash, R. D. M., Valencia, A. H. and Geffen, A. J. (2006). The origin of Fulton's condition factor – setting the record straight. *Fisheries* **31**, 236-238.
- Norin, T. and Metcalfe, N. B. (2019). Ecological and evolutionary consequences of metabolic rate plasticity in response to environmental change. *Philos. Trans. R. Soc. B Biol. Sci.* **374**, 20180180. doi:10.1098/rstb.2018.0180
- Pettersen, A. K. and Metcalfe, N. B. (2024). Consequences of the cost of living: Is variation in metabolic rate evolutionarily significant? *Philos. Trans. R. Soc. B Biol. Sci.* **379**, 20220498. doi:10.1098/rstb.2022.0498
- Pichaud, N., Ekström, A., Hellgren, K. and Sandblom, E. (2017). Dynamic changes in cardiac mitochondrial metabolism during warm acclimation in rainbow trout. *J. Exp. Biol.* **220**, 1674-1683. doi:10.1242/jeb.152421
- Pichaud, N., Ekström, A., Breton, S., Sundström, F., Rowinski, P., Blier, P. U. and Sandblom, E. (2019). Cardiac mitochondrial plasticity and thermal sensitivity in a fish inhabiting an artificially heated ecosystem. *Sci. Rep.* **9**, 17832. doi:10.1038/s41598-019-54165-3
- Queiros, Q., McKenzie, D. J., Dutto, G., Killen, S., Sarau, C. and Schull, Q. (2024). Fish shrinking, energy balance and climate change. *Sci. Total Environ.* **906**, 167310. doi:10.1016/j.scitotenv.2023.167310
- Rácz, A., Allan, B., Dwyer, T., Thambithurai, D., Crespel, A. and Killen, S. S. (2021). Identification of individual Zebrafish (Danio rerio): a refined protocol for VIE tagging whilst considering animal welfare and the principles of the 3Rs. *Animals* **11**, 616. doi:10.3390/ani11030616
- Rich, P. R. and Maréchal, A. (2010). The mitochondrial respiratory chain. *Essays Biochem.* **47**, 1-23. doi:10.1042/bse0470001
- Roussel, D. and Voituron, Y. (2020). Mitochondrial costs of being hot: Effects of acute thermal change on liver bioenergetics in toads (*Bufo bufo*). *Front. Physiol.* **11**, 153. doi:10.3389/fphys.2020.00153
- Roussel, D., Janillon, S., Teulier, L. and Pichaud, N. (2023). Succinate oxidation rescues mitochondrial ATP synthesis at high temperature in *Drosophila melanogaster*. *FEBS Lett.* **597**, 2221-2229. doi:10.1002/1873-3468.14701
- Salin, K., Luquet, E., Rey, B., Roussel, D. and Voituron, Y. (2012). Alteration of mitochondrial efficiency affects oxidative balance, development and growth in frog (*Rana temporaria*) tadpoles. *J. Exp. Biol.* **215**, 863-869. doi:10.1242/jeb.062745
- Salin, K., Auer, S. K., Rey, B., Selman, C. and Metcalfe, N. B. (2015). Variation in the link between oxygen consumption and ATP production, and its relevance for animal performance. *Proc. R. Soc. B* **282**, 20151028. doi:10.1098/rspb.2015.1028
- Sandblom, E., Clark, T. D., Gräns, A., Ekström, A., Brijis, J., Sundström, L. F., Odelström, A., Adill, A., Aho, T. and Jutfelt, F. (2016). Physiological constraints to climate warming in fish follow principles of plastic floors and concrete ceilings. *Nat. Commun.* **7**, 11447. doi:10.1038/ncomms11447
- Schulte, P. M., Healy, T. M. and Fangué, N. A. (2011). Thermal performance curves, phenotypic plasticity, and the time scales of temperature exposure. *Integr. Comp. Biol.* **51**, 691-702. doi:10.1093/icb/ict097
- Seebacher, F., Brand, M. D., Else, P. L., Guderley, H., Hulbert, A. J. and Moyes, C. D. (2010). Plasticity of oxidative metabolism in variable climates: molecular mechanisms. *Physiol. Biochem. Zool.* **83**, 721-732. doi:10.1086/649964
- Seebacher, F., White, C. R. and Franklin, C. E. (2015). Physiological plasticity increases resilience of ectothermic animals to climate change. *Nat. Clim. Change* **5**, 61-66. doi:10.1038/nclimate2457
- Singer, M. (2007). Mitochondrial function in sepsis: Acute phase versus multiple organ failure. *Crit. Care Med.* **35** Suppl., S441-S448. doi:10.1097/01.CCM.0000278049.48333.78
- Sokolova, I. (2021). Bioenergetics in environmental adaptation and stress tolerance of aquatic ectotherms: linking physiology and ecology in a multi-stressor landscape. *J. Exp. Biol.* **224** Suppl. 1, jeb236802. doi:10.1242/jeb.236802
- Svendsen, M. B. S., Bushnell, P. G. and Steffensen, J. F. (2016). Design and setup of intermittent-flow respirometry system for aquatic organisms. *J. Fish Biol.* **88**, 26-50. doi:10.1111/jfb.12797
- Teulier, L., Thoral, E., Queiros, Q., McKenzie, D. J., Roussel, D., Dutto, G., Gasset, E., Bourjea, J. and Sarau, C. (2019). Muscle bioenergetics of two emblematic Mediterranean fish species: *Sardina pilchardus* and *Sparus aurata*. *Comp. Biochem. Physiol. A Mol. Integr. Physiol.* **235**, 174-179. doi:10.1016/j.cbpa.2019.06.008
- Thoral, E., Farhat, E., Roussel, D., Cheng, H., Guillard, L., Pamentier, M. E., Weber, J.-M. and Teulier, L. (2022a). Different patterns of chronic hypoxia lead to hierarchical adaptive mechanisms in goldfish metabolism. *J. Exp. Biol.* **225**, jeb243194. doi:10.1242/jeb.243194
- Thoral, E., Roussel, D., Quispe, L., Voituron, Y. and Teulier, L. (2022b). Absence of mitochondrial responses in muscles of zebrafish exposed to several heat

- waves. *Comp. Biochem. Physiol. A Mol. Integr. Physiol.* **274**, 111299. doi:10.1016/j.cbpa.2022.111299
- Thoral, E., Roussel, D., Gasset, E., Dutto, G., Queiros, Q., McKenzie, D. J., Bourdeix, J.-H., Metral, L., Saraux, C. and Teulier, L.** (2023). Temperature-dependent metabolic consequences of food deprivation in the European sardine. *J. Exp. Biol.* **226**, jeb244984. doi:10.1242/jeb.244984
- Thoral, E., Dawson, N. J., Bettinazzi, S. and Rodríguez, E.** (2024). An evolving roadmap: Using mitochondrial physiology to help guide conservation efforts. *Conserv. Physiol.* **12**, coae063. doi:10.1093/conphys/coae063
- Voituron, Y., Roussel, D., Le Galliard, J.-F., Dupoué, A., Romestaing, C. and Meylan, S.** (2022a). Mitochondrial oxidative phosphorylation response overrides glucocorticoid-induced stress in a reptile. *J. Comp. Physiol. B* **192**, 765-774. doi:10.1007/s00360-022-01454-5
- Voituron, Y., Roussel, D., Teulier, L., Vagner, M., Ternon, Q., Romestaing, C., Dubillot, E. and Lefrançois, C.** (2022b). Warm acclimation increases mitochondrial efficiency in fish: a compensatory mechanism to reduce the demand for oxygen. *Physiol. Biochem. Zool.* **95**, 15-21. doi:10.1086/716904



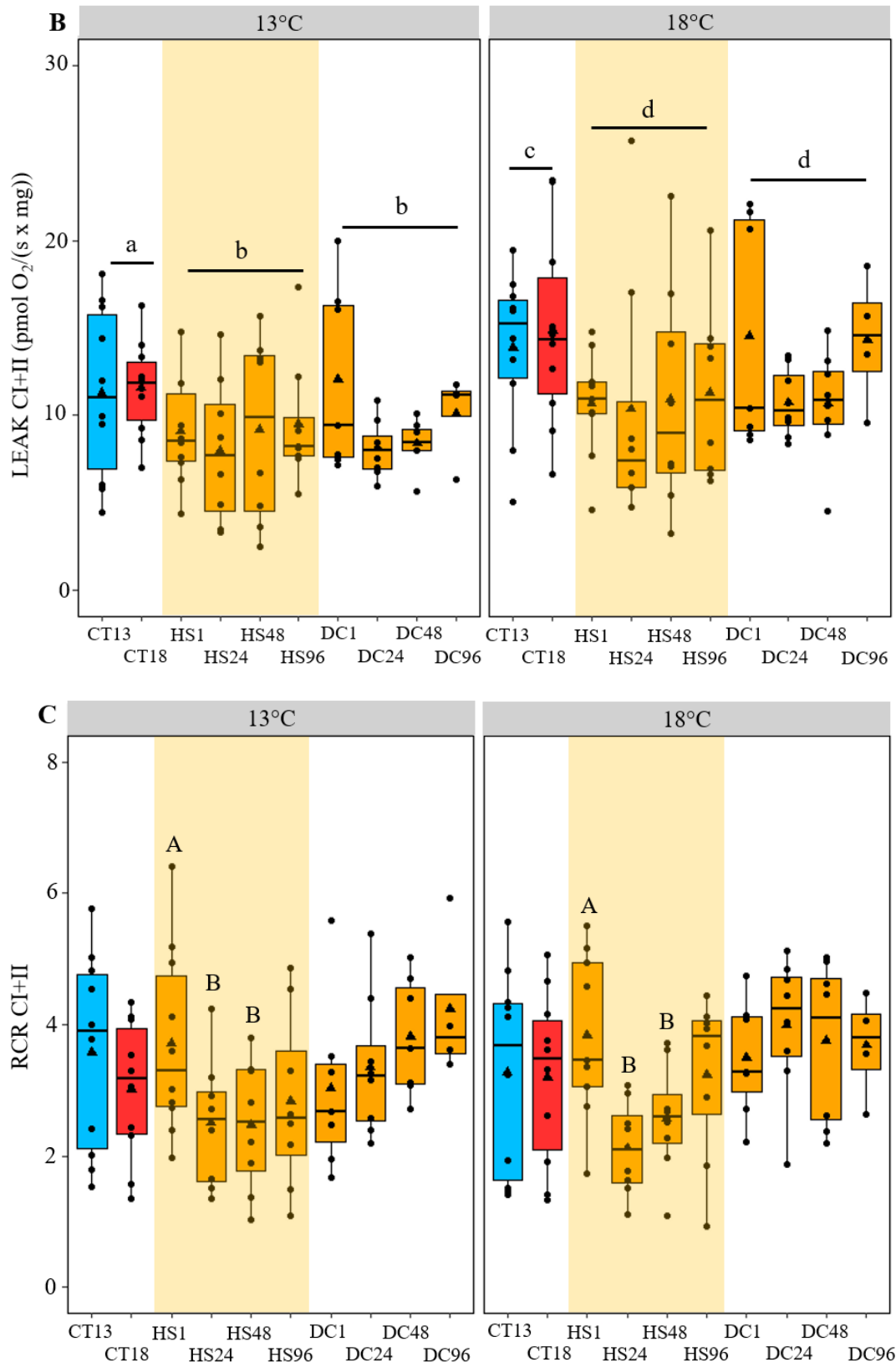


**Fig. S1: Mitochondrial respiration rates among the different experimental groups and depending on assay temperature.** Different respiration rates are represented, and all values are in pmol O<sub>2</sub>(s x mg) of heart. OXPHOS CI+II (A), LEAK CI+II (B) and RCR CI+II (C). Different colors indicate different treatment groups: the CT13 group is in blue, the CT18 group in red and the HS1 – HS24 – HS48 – HS96 – DC1 – DC24 – DC48 – DC96. The circles represent individual values, the triangles on the boxplot represent the mean and the orange box represents the interval of the heat stress. For the sake of visibility, the scales are not the same for each graph. n = 4 – 10 for each group. Different letters indicate a significant difference between the groups tested with the “phase” method where the CT, HS and DC phases were tested for differences among each other. In panel C, different capital letters indicate a significant difference between individual groups. All differences are p<0.05 according to post-hoc tests corrected with Tukey’s method.

### Statistics tables

For each mitochondrial parameter, there is the table with the linear (mixed) model (“LM”) and the tables for the method with pooled groups. For this method, the “CT”, “HS” and “DC” tables are to see if there are any differences among the CT13 and CT18 groups, among the HS1, HS24, HS48 and HS96 groups and among the DC1, DC24, DC48 and DC96 respectively. Then the “CT-HS”, “CT-DC” and “DC-HS” tables compare each set of pooled groups among each other. In the tables, “temp” means assay temperature, “trt” means treatment group and “bm” means body mass.

**Table S1. Statistics tables for OXPHOS CI (A), OXPHOS CI+II (B), LEAK CI (C) and LEAK CI+II (D) mitochondrial respiration**

#### A) OXPHOS CI

OXPHOS CI	CT					
Anova	sum sq	mean sq	num df	den df	F value	Pr (>F)
trt	310,010	310,010	1	17	1,603	0,223
temp	519,370	519,370	1	19	2,686	0,118
bm	1024,670	1024,670	1	17	5,300	0,034
	HS					
Anova	sum sq	mean sq	num df	den df	F value	Pr (>F)
trt	1125,820	375,270	3	28,878	2,700	0,064
temp	1503,140	1503,140	1	32,086	10,814	0,002
bm	50,350	50,350	1	28,445	0,362	0,552
	DC					
Anova	sum sq	mean sq	num df	den df	F value	Pr (>F)
trt	319,230	106,410	3	22	1,008	0,408
temp	1743,390	1743,390	1	26	16,509	0,0004
bm	59,450	59,450	1	22	0,563	0,461

OXPHOS CI	CT-HS					
Anova	sum sq	mean sq	num df	den df	F value	Pr (>F)
phase	1244,090	1244,090	1	51,077	7,974	0,007
temp	1906,120	1906,120	1	52,554	12,217	0,001
bm	685,950	685,950	1	50,766	4,397	0,041
OXPHOS CI	CT-DC					
Anova	sum sq	mean sq	num df	den df	F value	Pr (>F)
phase	114,060	114,060	1	44	0,805	0,375
temp	2163,480	2163,480	1	46	15,267	0,0003
bm	880,900	880,900	1	44	6,216	0,016
OXPHOS CI	DC-HS					
Anova	sum sq	mean sq	num df	den df	F value	Pr (>F)
phase	695,960	695,960	1	58,274	5,721	0,020
temp	3123,000	3123,000	1	59,534	25,673	4,199E-06
bm	160,560	160,560	1	57,8	1,320	0,255

OXPHOS CI	LM					
Anova	sum sq	mean sq	num df	den df	F value	Pr (>F)
trt	3041,000	337,900	9	69,838	2,433	0,018
temp	3665,600	3665,600	1	79,035	26,398	1,96E-06
bm	875,100	875,100	1	69,363	6,302	0,014

## B) OXPBOS CI+II

OXPHOS CI+II	CT					
Anova	sum sq	mean sq	num df	den df	F value	Pr (>F)
trt	425,81	425,81	1	17	1,435	0,247
temp	1109,44	1109,44	1	19	3,739	0,068
bm	1339,89	1339,89	1	17	4,516	0,049
OXPHOS CI+II	HS					
Anova	sum sq	mean sq	num df	den df	F value	Pr (>F)
trt	1340,530	446,840	3	29,203	2,174	0,112
temp	1462,690	1462,690	1	32,424	7,116	0,012
bm	292,330	292,330	1	28,766	1,422	0,243
OXPHOS CI+II	DC					
Anova	sum sq	mean sq	num df	den df	F value	Pr (>F)
trt	291,390	97,130	3	22	0,681	0,573
temp	2015,780	2015,780	1	26	14,122	8,760E-04
bm	1,520	1,520	1	22	0,011	0,919

OXPHOS CI+II		CT-HS					
Anova	sum sq	mean sq	num df	den df	F value	Pr (>F)	
phase	2203,800	2203,800	1	51,087	9,382	0,003	
temp	2457,700	2457,700	1	52,665	10,463	0,002	
bm	1085,000	1085,000	1	50,762	4,619	0,036	
		CT-DC					
Anova	sum sq	mean sq	num df	den df	F value	Pr (>F)	
phase	218,320	218,320	1	44	1,072	0,306	
temp	3108,880	3108,880	1	46	15,270	0,0003	
bm	811,850	811,850	1	44	3,988	0,052	
		DC-HS					
Anova	sum sq	mean sq	num df	den df	F value	Pr (>F)	
phase	996,000	996,000	1	58,259	5,693	0,020	
temp	3300,100	3300,100	1	59,567	18,862	5,542E-05	
bm	164,200	164,200	1	57,774	0,939	0,337	
OXPHOS CI+II		LM					
Anova	sum sq	mean sq	num df	den df	F value	Pr (>F)	
trt	4011,400	445,700	9	70,197	2,202	0,032	
temp	4524,900	4524,900	1	79,424	22,356	9,66E-06	
bm	1044,700	1044,700	1	69,715	5,161	0,026	

C) LEAK CI

LEAK CI		CT					
Anova	sum sq	mean sq	num df	den df	F value	Pr (>F)	
trt	3,443	3,443	1	17	2,253	0,152	
temp	5,902	5,902	1	19	3,862	0,064	
bm	8,476	8,476	1	17	5,546	0,031	
		HS					
Anova	sum sq	mean sq	num df	den df	F value	Pr (>F)	
trt	8,657	2,886	3	28,703	0,908	0,449	
temp	52,512	52,512	1	32,240	16,525	0,0003	
bm	1,177	1,177	1	28,218	0,370	0,548	
		DC					
Anova	sum sq	mean sq	num df	den df	F value	Pr (>F)	
trt	8,719	2,906	3	22	1,919	0,156	
temp	24,885	24,885	1	26	16,428	0,0004	
bm	4,554	4,554	1	22	3,003	0,097	

LEAK CI		CT-HS					
Anova	sum sq	mean sq	num df	den df	F value	Pr (>F)	
phase	35,332	35,332	1	50,801	13,444	0,001	
temp	52,522	52,522	1	51,954	19,985	4,261E-05	
bm	15,211	15,211	1	50,542	5,788	0,020	
		CT-DC					
Anova	sum sq	mean sq	num df	den df	F value	Pr (>F)	
phase	8,789	8,789	1	44	5,742	0,021	
temp	28,791	28,791	1	46	18,808	7,814E-05	
bm	16,904	16,904	1	44	11,043	0,002	
		DC-HS					
Anova	sum sq	mean sq	num df	den df	F value	Pr (>F)	
phase	6,874	6,874	1	57,76	2,859	0,096	
temp	77,184	77,184	1	58,976	32,011	4,609E-07	
bm	28,473	28,473	1	57,298	11,842	0,001	
LEAK CI		LM					
Anova	sum sq	mean sq	num df	den df	F value	Pr (>F)	
trt	61,945	6,883	9	69,989	3,093	0,003	
temp	76,720	76,720	1	78,801	34,476	9,76E-08	
bm	24,989	24,989	1	69,624	11,229	0,001	

#### D) LEAK CI+II

LEAK CI+II		CT					
Anova	sum sq	mean sq	num df	den df	F value	Pr (>F)	
trt	35,012	35,012	1	17	3,171	0,093	
temp	84,573	84,573	1	19	7,660	0,012	
bm	47,863	47,863	1	17	4,335	0,053	
		HS					
Anova	sum sq	mean sq	num df	den df	F value	Pr (>F)	
trt	5,619	1,873	3	28,970	0,187	0,905	
temp	69,787	69,787	1	31,853	6,956	0,0128	
bm	27,525	27,525	1	28,612	2,744	0,109	
LEAK CI+II		DC					
Anova	sum sq	mean sq	num df	den df	F value	Pr (>F)	
trt	5,677	1,892	3	21,685	0,947	0,435	
temp	88,106	88,106	1	24,874	44,106	6,008E-07	
bm	2,915	2,915	1	22,168	1,459	0,240	

LEAK CI+II	CT-HS					
Anova	sum sq	mean sq	num df	den df	F value	Pr (>F)
phase	92,159	92,159	1	50,546	8,949	0,004
temp	148,358	148,358	1	51,917	14,406	3,869E-04
bm	27,858	27,858	1	50,251	2,705	0,106
	CT-DC					
Anova	sum sq	mean sq	num df	den df	F value	Pr (>F)
phase	28,328	28,328	1	43,943	4,891	0,032
temp	175,019	175,019	1	45,147	30,215	1,717E-06
bm	27,629	27,629	1	44,557	4,770	0,034
	DC-HS					
Anova	sum sq	mean sq	num df	den df	F value	Pr (>F)
phase	11,964	11,964	1	56,989	1,866	0,177
temp	159,758	159,758	1	57,304	24,911	5,9300E-06
bm	47,369	47,369	1	59,452	7,386	0,009
LEAK CI+II	LM					
Anova	sum sq	mean sq	num df	den df	F value	Pr (>F)
trt	138,851	15,428	9	69,235	2,056	0,046
temp	242,487	242,487	1	77,480	32,312	2,21E-07
bm	61,285	61,285	1	69,822	8,166	0,006

**Table S2. Statistics tables for cAS CI, cAS CI+II, RCR CI and RCR CI+II mitochondrial respiration**

**A) cAS CI**

cAS CI		CT					
Anova	sum sq	mean sq	num df	den df	F value	Pr (>F)	
trt	166,46	166,46	1	17	0,940	0,346	
temp	414,54	141,54	1	19	2,341	0,142	
bm	594,76	594,76	1	17	3,359	0,084	
		HS					
Anova	sum sq	mean sq	num df	den df	F value	Pr (>F)	
trt	1232,260	410,750	3	28,823	3,255	0,036	
temp	998,260	998,260	1	32,071	7,912	0,008	
bm	40,140	40,140	1	28,383	0,318	0,577	
		DC					
Anova	sum sq	mean sq	num df	den df	F value	Pr (>F)	
trt	200,150	66,720	3	22	0,711	0,556	
temp	1351,690	1351,690	1	26	14,408	7,946E-04	
bm	21,100	21,100	1	22	0,225	0,640	
cAS CI		CT-HS					
Anova	sum sq	mean sq	num df	den df	F value	Pr (>F)	
phase	768,350	768,350	1	51,131	5,420	0,024	
temp	1323,000	1323,000	1	52,573	9,332	3,531E-03	
bm	448,090	448,090	1	50,826	3,161	0,081	
		CT-DC					
Anova	sum sq	mean sq	num df	den df	F value	Pr (>F)	
phase	26,890	26,890	1	44	0,210	0,649	
temp	1693,110	1693,110	1	46	13,252	6,8760E-04	
bm	465,670	465,670	1	44	3,645	0,063	
		DC-HS					
Anova	sum sq	mean sq	num df	den df	F value	Pr (>F)	
phase	555,390	555,390	1	58,334	5,062	0,028	
temp	2217,570	2217,570	1	59,584	20,212	3,26E-05	
bm	51,250	51,250	1	57,862	0,467	0,497	
cAS CI		LM					
Anova	sum sq	mean sq	num df	den df	F value	Pr (>F)	
trt	2361,380	262,430	9	69,872	2,089	0,042	
temp	2676,800	2676,800	1	79,036	21,312	1,49E-05	
bm	517,650	517,650	1	69,405	4,121	0,046	

**B) cAS CI + CII**

cAS CI+II	CT						
Anova	sum sq	mean sq	num df	den df	F value	Pr (>F)	
trt	177,85	177,85	1	17	0,848	0,370	
temp	581,39	581,39	1	19	2,772	0,112	
bm	725,52	725,52	1	17	3,460	0,080	
HS							
Anova	sum sq	mean sq	num df	den df	F value	Pr (>F)	
trt	1365,080	455,030	3	29,074	3,006	0,046	
temp	906,770	906,770	1	32,433	5,990	0,200	
bm	132,930	132,930	1	28,214	0,878	0,357	
DC							
Anova	sum sq	mean sq	num df	den df	F value	Pr (>F)	
trt	202,620	67,540	3	22	0,563	0,645	
temp	1141,910	1141,910	1	26	9,520	4,778E-03	
bm	21,860	21,860	1	22	0,182	0,674	
CT-HS							
Anova	sum sq	mean sq	num df	den df	F value	Pr (>F)	
phase	1272,370	1272,370	1	51,164	7,512	0,008	
temp	1399,990	1399,990	1	52,708	8,265	5,817E-03	
bm	709,230	709,230	1	50,843	4,187	0,046	
CT-DC							
Anova	sum sq	mean sq	num df	den df	F value	Pr (>F)	
phase	43,850	43,850	1	44	0,283	0,597	
temp	1709,090	1709,090	1	46	11,046	1,7500E-03	
bm	385,340	385,340	1	44	2,491	0,122	
DC-HS							
Anova	sum sq	mean sq	num df	den df	F value	Pr (>F)	
phase	834,340	834,340	1	58,358	6,189	0,016	
temp	1923,350	1923,350	1	59,764	14,267	3,68E-04	
bm	4,580	4,580	1	57,85	0,034	0,854	
LM							
Anova	sum sq	mean sq	num df	den df	F value	Pr (>F)	
trt	2830,870	314,540	9	70,135	2,074	0,044	
temp	2589,470	2589,470	1	79,373	17,075	8,84E-05	
bm	472,390	472,390	1	69,650	3,115	0,082	

C) RCR CI

RCR CI		CT					
Anova	sum sq	mean sq	num df	den df	F value	Pr (>F)	
trt	3,562	3,562	1	17	0,240	0,631	
temp	0,942	0,942	1	19	0,063	0,804	
bm	2,61	2,61	1	17	0,176	0,680	
		HS					
Anova	sum sq	mean sq	num df	den df	F value	Pr (>F)	
trt	89,334	29,778	3	28,639	4,184	0,014	
temp	7,508	7,507	1	31,402	1,055	0,312	
bm	2,940	2,940	1	28,316	0,413	0,526	
		DC					
Anova	sum sq	mean sq	num df	den df	F value	Pr (>F)	
trt	5,677	1,892	3	22	0,521	0,672	
temp	6,295	6,295	1	26	1,734	0,199	
bm	1,330	1,330	1	22	0,366	0,551	

RCR CI		CT-HS					
Anova	sum sq	mean sq	num df	den df	F value	Pr (>F)	
phase	0,111	0,111	1	51,117	0,011	0,916	
temp	9,239	9,239	1	52,365	0,943	0,336	
bm	0,050	0,050	1	50,842	0,005	0,943	
		CT-DC					
Anova	sum sq	mean sq	num df	den df	F value	Pr (>F)	
phase	10,105	10,105	1	44	1,216	0,276	
temp	1,609	1,609	1	46	0,194	0,662	
bm	9,528	9,528	1	44	1,147	0,290	
		DC-HS					
Anova	sum sq	mean sq	num df	den df	F value	Pr (>F)	
phase	4,098	4,098	1	58,233	0,723	0,399	
temp	0,378	0,378	1	58,923	0,067	0,797	
bm	6,736	6,736	1	57,933	1,189	0,280	

RCR CI		LM					
Anova	sum sq	mean sq	num df	den df	F value	Pr (>F)	
trt	144,119	16,013	9	69,706	2,038	0,047	
temp	0,571	0,571	1	78,632	0,073	0,789	
bm	0,833	0,833	1	69,305	0,106	0,746	

D) RCR CI+II

RCR CI+II		CT					
Anova	sum sq	mean sq	num df	den df	F value	Pr (>F)	
trt	0,151	0,015	1,000	17,000	0,177	0,679	
temp	0,041	0,041	1,000	19,000	0,048	0,829	
bm	1,143	1,143	1,000	17,000	1,334	0,264	
		HS					
Anova	sum sq	mean sq	num df	den df	F value	Pr (>F)	
trt	7,722	2,574	3,000	28,648	3,653	0,024	
temp	0,048	0,048	1,000	31,713	0,068	0,796	
bm	0,028	0,028	1,000	28,246	0,040	0,842	
		DC					
Anova	sum sq	mean sq	num df	den df	F value	Pr (>F)	
trt	1,264	0,422	3,000	22,000	0,430	0,733	
temp	0,467	0,467	1,000	26,000	0,477	0,496	
bm	3,179	3,179	1,000	22,000	3,244	0,084	

RCR CI+II		CT-HS					
Anova	sum sq	mean sq	num df	den df	F value	Pr (>F)	
phase	1,170	1,170	1	51,125	1,577	0,215	
temp	0,001	0,001	1	52,366	0,002	9,658E-01	
bm	0,766	0,766	1	50,851	1,032	0,314	
		CT-DC					
Anova	sum sq	mean sq	num df	den df	F value	Pr (>F)	
phase	1,410	1,410	1	43,893	1,530	0,223	
temp	0,176	0,176	1	45,296	0,191	0,664	
bm	0,054	0,054	1	44,801	0,058	0,810	
		DC-HS					
Anova	sum sq	mean sq	num df	den df	F value	Pr (>F)	
phase	5,134	5,134	1	58,317	6,342	0,015	
temp	0,276	0,276	1	59,462	0,341	0,561	
bm	2,544	2,544	1	61,893	3,142	0,081	

RCR CI+II		LM					
Anova	sum sq	mean sq	num df	den df	F value	Pr (>F)	
trt	16,854	1,873	9	69,427	2,281	0,026	
temp	0,210	0,210	1	78,194	0,255	0,615	
bm	0,004	0,004	1	70,189	0,005	0,946	

**Table S3. Statistics tables for COX activity**

COX		CT					
Anova	sum sq	mean sq	num df	den df	F value	Pr (>F)	
trt	5,3	5,3	1	17	0,0115	0,916	
temp	7270,3	7270,3	1	19	15,874	0,001	
bm	409	409	1	17	0,893	0,358	
COX		HS					
Anova	sum sq	mean sq	num df	den df	F value	Pr (>F)	
trt	10094,200	3364,700	3	27,224	6,685	0,002	
temp	6032,500	6032,500	1	28,791	11,984	0,002	
bm	272,200	272,200	1	26,557	0,541	0,469	
COX		DC					
Anova	sum sq	mean sq	num df	den df	F value	Pr (>F)	
trt	2595,000	865,000	3	20,805	2,244	0,113	
temp	9056,200	9056,200	1	24,534	23,490	5,807E-05	
bm	238,300	238,300	1	20,701	0,618	0,441	

COX		CT-HS					
Anova	sum sq	mean sq	num df	den df	F value	Pr (>F)	
phase	57,500	57,500	1	48,374	0,119	0,732	
temp	12845,200	12845,200	1	47,941	26,603	4,713E-06	
bm	776,300	776,300	1	47,885	1,608	0,211	
COX		CT-DC					
Anova	sum sq	mean sq	num df	den df	F value	Pr (>F)	
phase	722,700	722,700	1	43,648	1,793	0,188	
temp	16583,300	16583,300	1	45,25	41,140	7,40E-08	
bm	1336,200	1336,200	1	43,78	3,315	0,076	
COX		DC-HS					
Anova	sum sq	mean sq	num df	den df	F value	Pr (>F)	
phase	382,600	382,600	1	54,786	0,854	0,360	
temp	14939,000	14939,000	1	53,421	33,331	4,02E-07	
bm	412,800	412,800	1	54,194	0,921	0,342	

COX		LM					
Anova	sum sq	mean sq	num df	den df	F value	Pr (>F)	
trt	12258,300	1362,000	9	67,618	3,073	0,004	
temp	22065,500	22065,500	1	74,598	49,783	7,47E-10	
bm	965,900	965,900	1	66,405	2,179	0,145	

**Table S4. statistics tables for OXPHOS CI, LEAK CI and AS CI normalized by COX**

**A) OXPHOS CI / COX**

OXPHOS CI		CT				
Anova	df	sum sq	mean sq	F	Pr (>F)	
trt	1	0,006	0,006		0,277	0,606
bm	1	0,142	0,142		6,674	0,019
Residual	17	0,362	0,021			
		HS				
Anova	df	sum sq	mean sq	F	Pr (>F)	
trt	3	0,078	0,026		1,343	0,274
bm	1	0,0001	0,0001		0,004	0,951
Residual	27	0,512	0,019			
		DC				
Anova	df	sum sq	mean sq	F	Pr (>F)	
trt	3	0,017	0,006		0,485	0,696
bm	1	0,006	0,006		0,505	0,485
Residual	21	0,246	0,012			

OXPHOS CI		CT-HS				
Anova	df	sum sq	mean sq	F	Pr (>F)	
phase	1	0,114	0,114		5,441	0,024
bm	1	0,077	0,077		3,708	0,060
Residual	49	1,023	0,021			
		CT-DC				
Anova	df	sum sq	mean sq	F	Pr (>F)	
phase	1	0,001	0,001		0,055	0,816
bm	1	0,085	0,849		5,255	0,027
Residual	43	0,695	0,162			
		DC-HS				
Anova	df	sum sq	mean sq	F	Pr (>F)	
phase	1	0,158	0,158		10,127	0,002
bm	1	0,001	0,001		0,064	0,801
Residual	55	0,857	0,016			

OXPHOS CI		LM				
Anova	df	sum sq	mean sq	F	Pr(>F)	
trt	9	0,294	0,033		1,860	0,073
bm	1	0,091	0,091		5,175	0,026
Residuals	67	1,178	0,018			

**B) LEAK CI / COX**

LEAK CI		CT				
Anova	df	sum sq	mean sq	F	Pr (>F)	
trt	1	0,003	0,003		0,793	0,386
bm	1	0,004	0,004		1,137	0,301
Residual	17	0,058	0,003			
		HS				
Anova	df	sum sq	mean sq	F	Pr (>F)	
trt	3	0,015	0,005		5,511	0,004
bm	1	0,0003	0,0003		0,356	0,556
Residual	27	0,025	0,001			
		DC				
Anova	df	sum sq	mean sq	F	Pr (>F)	
trt	3	0,002	0,001		1,078	0,380
bm	1	0,0002	0,0002		0,328	0,573
Residual	21	0,015	0,001			

LEAK CI		CT-HS				
Anova	df	sum sq	mean sq	F	Pr (>F)	
phase	1	0,002	0,002	0,986	0,326	
bm	1	0,005	0,005	2,395	0,128	
Residual	49	0,100	0,002			
		CT-DC				
Anova	df	sum sq	mean sq	F	Pr (>F)	
phase	1	0,001	0,001	0,627	0,433	
bm	1	0,007	0,007	4,323	0,044	
Residual	43	0,074	0,002			
		DC-HS				
Anova	df	sum sq	mean sq	F	Pr (>F)	
phase	1	0,0001	0,0001	0,126	0,724	
bm	1	0,001	0,001	0,597	0,443	
Residual	55	0,057	0,001			
LEAK CI		LM				
Anova	df	sum sq	mean sq	F	Pr(>F)	
trt	9	0,022	0,025	1,663	0,116	
bm	1	0,002	0,002	1,278	0,262	
Residuals	67	0,100	0,001			